Toxicology and Applied Pharmacology 424 (2021) 115598

Contents lists available at ScienceDirect

Toxicology and Applied Pharmacology

journal homepage: www.elsevier.com/locate/taap

Final results from a 90-day quantitative inhalation toxicology study evaluating the dose-response and fate in the lung and pleura of chrysotile-containing brake dust compared to TiO_2, chrysotile, crocidolite or amosite asbestos: Histopathological examination, confocal microscopy and collagen quantification of the lung and pleural cavity

David M. Bernstein [a,*], Balazs Toth [b], Rick A. Rogers [c], Peter Kunzendorf [d], James I. Phillips [e], Dirk Schaudien [f]

[a] Consultant in Toxicology, 40 ch de la Petite-Boissière, 1208 Geneva, Switzerland
[b] Charles River Laboratories Hungary Kft., Szabadságpuszta, Veszprém 8200, Hungary
[c] Rogers Imaging, 17 Erie Dr, Natick, MA 01760-1312, USA
[d] GSA Gesellschaft für Schadstoffanalytik mbH, Christinenstrasse 3, D-40880 Ratingen, Germany
[e] National Institute for Occupational Health, National Health Laboratory Service, Johannesburg South Africa and Department of Biomedical Technology, Faculty of Health Sciences, University of Johannesburg, Johannesburg 2000, South Africa
[f] Fraunhofer Institute for Toxicology and Experimental Medicine, 1 Nikolai-Fuchs-Strasse, D-30625 Hannover, Germany

ARTICLE INFO

Editor: Dr. Lawrence Lash

Keywords:
Brake dust
Chrysotile
Amphibole
Asbestos
Inhalation
Tumors
Pathology

ABSTRACT

The final results from this multi-dose, 90-day inhalation toxicology study in the rat with life-time post-exposure observation have shown a significant fundamental difference in pathological response and tumorgenicity between brake dust generated from brake pads manufactured with chrysotile or from chrysotile alone in comparison to the amphiboles, crocidolite and amosite asbestos.

The groups exposed to brake dust showed no significant pathological or tumorigenic response in the respiratory track compared to the air control group at exposure concentrations and deposited doses well above those at which humans have been exposed. Slight alveolar/interstitial macrophage accumulation of particles was noted. Wagner grades were 1–2 (1 = control group), similar to the TiO_2 particle control group.

Chrysotile was not biopersistent, exhibiting in the lung a deterioration of its matrix which results in breakage into particles and short fibers which can be cleared by alveolar macrophages and which can continue to dissolve. Particle-laden macrophage accumulation was observed, leading to a very-slight interstitial inflammatory response (Wagner grade 1–3). There was no peribronchiolar inflammation, occasional very-slight interstitial fibrosis (Wagner grade 4), and no exposure-related tumorigenic response.

The pathological response of crocidolite and amosite compared to the brake dust and chrysotile was clearly differentiated by the histopathology and the confocal analysis. Crocidolite and amosite induced persistent inflammation, microgranulomas, persistent fibrosis (Wagner grades 4), and a dose-related lung tumor response. Confocal microscopy quantified extensive inflammatory response and collagen development in the lung, visceral and parietal pleura as well as pleural adhesions.

These results provide a clear foundation for differentiating the innocuous effects of brake dust exposure from the adverse effects following amphibole asbestos exposure.

* Corresponding author.
E-mail addresses: davidb@itox.ch (D.M. Bernstein), Balazs.Toth@crl.com (B. Toth), rarogers5@yahoo.com (R.A. Rogers), kunzendorf@gsas.ch (P. Kunzendorf), jimphillipsy@gmail.com (J.I. Phillips), dirk.schaudien@item.fraunhofer.de (D. Schaudien).

https://doi.org/10.1016/j.taap.2021.115598
Received 15 March 2021; Received in revised form 24 May 2021; Accepted 27 May 2021
Available online 30 May 2021

1. Introduction

This study was designed to evaluate the hypothesis of whether dust generated from brake drums with chrysotile in the matrix can produce a pathological/tumorigenic response following 90-day sub-chronic inhalation exposure in rats with a post-exposure observation period through the rat's life-time[1]. For comparison, low toxicity particle (TiO_2) and chrysotile and amphibole asbestos control groups were included. In earlier inhalation toxicology studies of brake dust which contained chrysotile with exposures of either 5 days (exposure concentration 46 WHO f/cm^3) or 28 days exposure (exposure concentrations 7, 15, 24 WHO f/cm^3) (Bernstein et al., 2014, 2015, 2018) brake dust was shown to produces no pathological response in the respiratory tract or pleura. Chrysotile alone (similar to that used in the brake dust) was shown to have minimal effect, whereas a significant pathological response in both the lung and pleural cavity was observed following exposure to the amphibole crocidolite asbestos in both the 5-day and 28-day studies.

The current study was designed to evaluate the exposure-response of brake dust manufactured with chrysotile in comparison to the particle control, TiO_2, 2 doses of a chrysotile similar to that used in the brake dust, and to the amphiboles crocidolite and amosite asbestos. Nine groups of CRL:WI Wistar Han male rats (Groups 1–9) were exposed for 13 weeks (5 days/week), 6 h per day followed by a post-exposure period through 24.4 months (~20 % survival). The study involved exposure by flow-past nose-only inhalation to 1020 rats (9 treatment groups, 106 animals per group) with 31 rats/group included in the final sacrifice which occurred at 24.4 months.

The 90-day sub-chronic inhalation toxicity study is often a pivotal study for assessing no-effect levels as well as longer-term toxicity. The protocol design for a regulatory sub-chronic 90-day inhalation toxicity study stipulates a post-exposure recovery period of up to four weeks (EPA 712–C–98–204; OECD 413, 2018). As there is a long latency period for fiber-related disease in humans, to fully evaluate the long-term ability of the test materials to cause disease, this study was designed with a lifetime post-exposure period.

The methods and interim results through 180 days (90 days post-exposure) have been presented in Bernstein et al., 2019a, 2019b. These include the results from the experimental design, aerosol exposure, lung burdens through 180 days, and the bronchoalveolar lavage results (Bernstein et al., 2019a). The methods for histopathological examination of the lungs and confocal microscopy examination of the lung and the pleural cavity, as well as the results through 90 days post-exposure were presented in Bernstein et al., 2019b. This included the histopathological quantification of fibrosis and the confocal microscopy quantification of collagen in the lung and pleura.

With the confocal microscopy examination and analysis *in situ* 3D images of the lung and pleural cavity and any associated pathology present were obtained. The number and length of fibers in these regions were also determined. The confocal methodology provided a fully quantitative assessment of the amount of collagen present in the lung and in the visceral and parietal pleura (Rogers, 1999).

To provide continuity with the interim results through 180 days (Bernstein et al., 2019a, 2019b) a similar format has been followed in this final publication.

2. Methods

The experimental design, study plan and timing of the exposure and post-exposure recovery period are summarized in Fig. 1. The solid time-line bar shows the study day. On top of the time-bar are shown the interim sacrifices. On the bottom of the time-bar the inhalation exposure period and the post-exposure recovery period are indicated. The results through 180 days (3 months post-exposure) including the BAL were presented in Bernstein et al. (2019a, 2019b).

Nine groups of laboratory rats were exposed by flow-past nose-only inhalation for 6 h per day 5 days per week for 13 weeks (Table 1). Subsets of animals were sacrificed immediately following 45 and 89 days of exposure (within ~ 0.2 to 1 h after exposure termination) and at 3, 6, 9, 12, 18 and 24 months following the last exposure (experimental day 180, 270, 360, 450, 540, 745). The final sacrifice occurred at day 745, (21.4 month after the last exposure) when the groups reached ~ 20 % survival. The following groups were exposed:

Analyses conducted for each group:

- Aerosol exposure characterization (Bernstein et al., 2019a)
- Fiber/Particle lung burden evaluation at 45 d, 89 d, 3 and 12 m (45 d, 89 d, 3 m presented in Bernstein et al., 2019a)
- Bronchoalveolar lavage examination at 45 d, 89 d, 3 and 12 m (presented in Bernstein et al., 2019a)
- Histopathology examination at 45 d, 89 d, 3, 6, 12, 18 and 24 m (the results through 180 days were presented in Bernstein et al., 2019b)
- Histopathology quantification of fibrosis at 45 d, 89 d, 3, 6, 12, 18 m.
- Confocal microscopy imaging of the lung, and quantification of collagen in the lung parenchyma at 45 & 89 d, 3, 6, 12, 18 & 24 m (the results through 180 d were presented in Bernstein et al., 2019b)
- Confocal low temperature microscopy imaging of the lung and chestwall, and quantification of collagen in the visceral and parietal pleura at 45 & 89 d, 3, 6, 12 & 18 m (the results through 180 d were presented in Bernstein et al., 2019b). The 24 m time point was not included in order to maximize the number of rats available for histopathological examination at the final sacrifice.

The methods for necropsy and histopathological examination and confocal microscopy imaging and collagen quantification have been presented previously (Bernstein et al., 2019b) and are included here in Section S-10 of the Supplemental data.

Titanium dioxide (TiO_2) was included as a low toxicity particle control. IARC (2010) has classified TiO_2 as a possible carcinogen. As stated in the IARC preamble, the IARC Monographs evaluate cancer hazards not risk. They further state that "Inclusion of an agent in the Monographs does not imply that it is a carcinogen, only that the published data have been examined". For the animal toxicology studies, the IARC classification was based on "lung overload" exposures at what would be considered very high exposure concentrations. Subsequently, ECETOC (2013) has evaluated the influence of lung overload on lung tumor formation and have concluded that "detailed epidemiological studies in TiO_2 and carbon black workers provide unequivocal evidence of no causal link between particle exposures and lung cancers or other non-neoplastic lung diseases".

We have included as part of the histopathological examination, grading the lungs using the Wagner grading system for pulmonary lesions (Wagner et al., 1974; McConnell et al., 1984). In a subsequent review of the Wagner grading system, McConnell and Davis (2002) explained that the system was not specific enough, as it "failed to quantitatively differentiate the magnitude of collagen deposition/early fibrosis as it relates to the amount of the lung involved in the fibrotic process. For example, an animal with only an occasional focus of fibrosis and one with numerous foci are both classified as Wagner Grade 4, although they are vastly different in terms of their overall pathology and impact on the pulmonary health of the animal. Because of this, the differential pathology of various types of fibers is diminished or lost with this approach." "The reason for developing a method for more precise quantification of Wagner Grade 4 fibrosis was that it was appreciated that the widely used Wagner scale did not differentiate between the presence of trivial amounts of fibrosis and more widespread fibrotic change." This more quantitative method which was proposed by McConnell and Davis (2002) which "quantifies the total area of the lung

[1] Lifetime exposure was defined as when ~20% of the rats in one of the exposure groups remained. In the study, all the exposure groups reached ~20% survival within the same time frame.

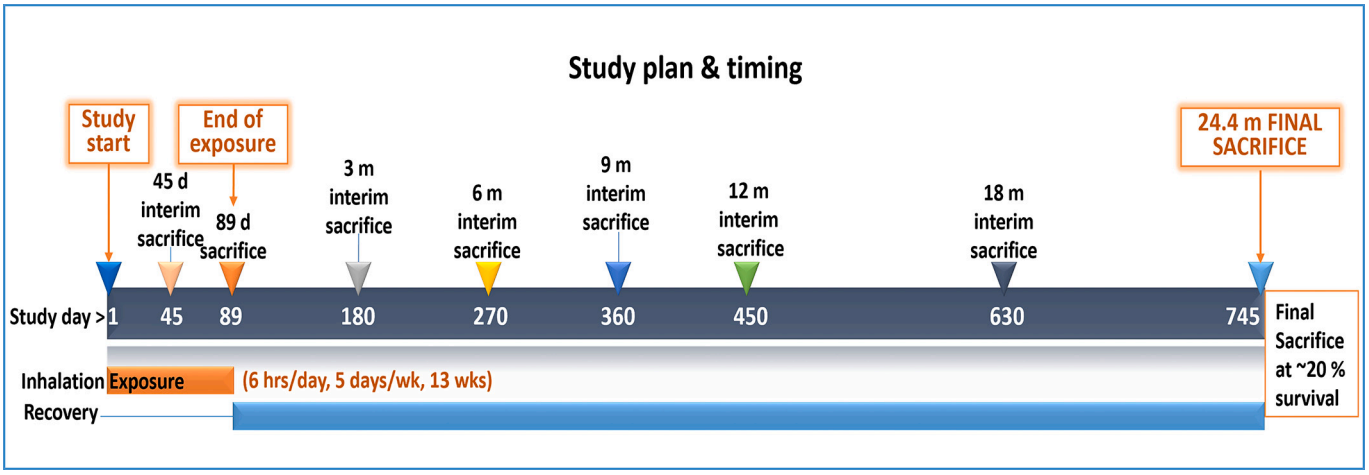

Fig. 1. Study plan and timing. Exposure was through day 89 (6 hrs/day, 5 days/wk, 13 wks). The final sacrifice was at 24.4 months (~20 % survival).

Table 1
Exposure groups, mean gravimetric and fiber concentrations (WHO fibers; Fibers L > 20 μm), geometric mean diameter (GMD) and geometric mean length (GML).

Exposure group	Mean gravimetric concentrations	Mean fiber concentrations		GMD	GML
	mg/m^3	WHO fibers/cm^3	fibers L > 20 μm/cm^3	μm (std dev)	μm (std dev)
Group 1: Air Control		0.2	0	0.27 (1.89)	1.58 (1–83)
Group 2: Low dose (LD) level of brake dust	0.20	2.4	0.2	0.15 (1.88)	1.72 (1.96)
Group 3: Mid dose (MD) level of brake dust	0.34	4.9	0.4	0.16 (1.73)	2.20 (2.05)
Group 4: High dose (HD) level of brake dust	0.67	6.6	0.5	0.15 (1.91)	1.86 (2.15)
Group 5: Titanium dioxide (TiO_2) particle control	0.70	0.3	0	0.23 (1.77)	1.31 (1.97)
Group 6: Low dose level of Chrysotile 7H19	0.27	119	28.4	0.11 (1.86)	2.52 (2.65)
Group 7: High dose level of Chrysotile 7H19	0.64	233	72.3	0.11 (1.85)	3.89 (3.31)
Group 8: High dose level of Crocidolite asbestos (Voorspoed mine)	1.28	181	23.5	0.24 (1.80)	3.72 (2.62)
Group 9: High dose level of Amosite asbestos	2.32	281	47.7	0.28 (1.80)	3.85 (2.80)

WHO fibers: WHO fibers are defined by the World Health Organization to have L > 5 μm, D < 3 μm and aspect ratio (L/D) of 3:1 (WHO, 1985; NIOSH, 1994). SD: Standard deviation; GMD: Geometric mean diameter; GML: Geometric mean length; MMAD: Mass median aerodynamic diameter.

showing fibrosis specifically as it relates to Wagner Grade 4 fibrosis" is included as well in this study.

3. Results

3.1. Fiber lung burden at 12 months[2]

The mean particle and fiber lung burden through 12 months (9 months post-exposure) are presented in section S-8 (Supplemental data). With the brake dust groups, no fibers with L > 20 μm remained at 12 months. In the chrysotile exposed groups, a mean of 3–5 fibers were observed on the filter sample corresponding to 40,000–70,000 fibers per lung. This is in contrast to the crocidolite and amosite asbestos exposed groups where approximately 10,500,000 fibers L > 20 μm per lung were observed at 12 months.

3.2. Lung weights

The terminal body weight and the lung weight of each animal at necropsy were measured and recorded. Table 2 summarizes the lung weight/body weight ratios. In Groups 8 and 9 at all time points (except 635 days, Group 8), statistically significant increases were seen of approximately 20 % compared to the control group, likely as a result of edema in response to the inflammation produced by the amphibole fibers. Statistical comparisons including ANOVA analysis are presented in Section S-1 (supplemental data).

4. Histopathology

The histopathology results are summarized below.

- The final histopathology report is presented in Section S-2 (Supplemental data);
- the histopathological images from each sacrifice are shown in Section S-3 (Supplemental data) and
- the detailed tables itemizing all of the histopathological findings in Section S-9 (Supplemental data).

4.1. Pathology review board

The findings as reported by Fraunhofer and the slides with lesions for

[2] Later time points were not included for fiber lung burden in order to maximize the number of rats/group at the final sacrifice.

Table 2
Lung weight/body weight (ratio) at necropsy (Means/Standard deviations (number of animals)).

Group	Clean air control	Brake dust low	Brake dust mid	Brake dust high	Titanium-dioxide	Chrysotile low	Chrysotile high	Crocidolite	Amosite
45 days									
Mean	**0.388**	**0.363**	**0.368**	**0.354**	**0.354**	**0.404**	**0.413**	**0.463***	**0.466***
Std. Dev (no)	0.035 (8)	0.052 (8)	0.032 (8)	0.018 (8)	0.037 (8)	0.033 (8)	0.035 (8)	0.074 (8)	0.048
89 days									
Mean	**0.386**	**0.346**	**0.360**	**0.376**	**0.348**	**0.378**	**0.368**	**0.448***	**0.462***
Std. Dev (no)	0.034 (5)	0.032 (5)	0.042 (5)	0.026 (5)	0.018 (5)	0.022 (5)	0.030 (5)	0.040 (5)	0.036 (5)
180 days									
Mean	**0.300**	**0.280**	**0.280**	**0.285**	**0.294**	**0.330**	**0.304**	**0.359***	**0.399***
Std. Dev (no)	0.031 (8)	0.038 (8)	0.050 (8)	0.041 (8)	0.025 (8)	0.035 (8)	0.017 (8)	0.051 (8)	0.023 (8)
270 days									
Mean	**0.310**	**0.325**	**0.298**	**0.320**	**0.305**	**0.325**	**0.320**	**0.388***	**0.370***
Std. Dev (no)	0.022 (4)	0.019 (4)	0.040 (4)	0.028 (4)	0.006 (4)	0.006 (4)	0.029 (4)	0.021 (4)	0.016 (4)
451 days									
Mean	**0.315**	**0.303**	**0.295**	**0.290**	**0.310**	**0.293**	**0.273**	**0.338***	**0.368***
Std. Dev (no)	0.066 (4)	0.058 (4)	0.017 (4)	0.027 (4)	0.035 (4)	0.022 (4)	0.035 (3)	0.024 (4)	0.021 (4)
635 days									
Mean	**0.303**	**0.327**	**0.287**	**0.328**	**0.300**	**0.290**	**0.290**	**0.350**	**0.417***
Std. Dev (no)	0.022 (4)	0.029 (3)	0.015 (3)	0.025 (4)	0.014 (4)	0.024 (4)	0.000 (1)	0.057 (4)	0.072 (3)
741 days									
Mean	**0.298**	**0.295**	**0.290**	**0.308**	**0.320**	**0.312**	**0.330**	**0.342***	**0.360***
Std. Dev (no)	0.047 (25)	0.045 (27)	0.052 (27)	0.026 (24)	0.070 (28)	0.042 (26)	0.036 (23)	0.090 (21)	0.052 (21)

Mean values are shown in bold.
* Dunnet's test/ANOVA, statistically significant compared to controls.

the final sacrifice were reviewed by an independent pathology review board. The board members are listed in the acknowledgments. All neoplastic and preneoplastic lesions were reviewed and the findings agreed upon by the board. The results presented herein fully reflect those findings.

4.2. Neoplastic findings

Tumors within the lung (Table 3) were detected in the groups: clean air (one tumor), brake dust high (one tumor), titanium dioxide (one tumor), chrysotile low (one tumor), crocidolite (five tumors), and amosite (nine tumors). These consisted of malignant tumors in one animal of group brake dust high (this animal had two bronchiolo-alveolar carcinomas), one malignant tumor in group titanium dioxide (bronchiolo-alveolar carcinoma), three malignant tumors in group crocidolite (all bronchiolo-alveolar carcinomas), and four malignant tumors in group amosite (three bronchiolo-alveolar carcinomas and one adenocarcinoma) and benign bronchiolo-alveolar adenomas in group clean air (one adenoma), chrysotile low (one adenoma), crocidolite (one adenoma and one adenoma with atypia), and amosite (four adenomas and one adenoma with atypia).

In addition, as shown in Table 4, bronchiolo-alveolar hyperplasias of the alveolar type with atypia (hyperplasia of type 2 pneumocytes) was observed in the groups: clean air (one), brake dust low (one), brake dust high (two), chrysotile high (one), crocidolite (four), and amosite (three). One of the three animals of the amosite group with the bronchiolo-alveolar hyperplasias of the alveolar type with atypia had two of these lesions. Bronchiolo-alveolar hyperplasias of the alveolar type without atypia (hyperplasia of type 2 pneumocytes) were observed in the groups: clean air (one), brake dust low (five), brake dust mid (one), brake dust high (four), titanium dioxide (three), chrysotile low (four), chrysotile high (seven), crocidolite (eight), and amosite (six). Bronchiolo-alveolar hyperplasias of the alveolar type were only diagnosed if they were not correlated to spontaneous alveolar macrophage aggregation.

Bronchiolo-alveolar hyperplasias of the bronchiolar type (bronchiolization) were diagnosed as "hyperplasia, bronchiolo-alveolar". These findings were interpreted to be an adaptive change. The spontaneous alveolar macrophage aggregation sometimes induced infiltration of inflammatory cells, minimal fibrosis and hyperplasia of type 2 pneumocytes, which was diagnosed as chronic inflammation. Since these spontaneous alveolar macrophage aggregations were sometimes localized subpleurally, there was sometimes a subpleurally localized chronic inflammation including a concurrent pleural fibrosis (Renne et al., 2009).

Metastases into the lung originating from primary tumors outside the respiratory tract as confirmed through organ examination were seen in one animal of group 1 (clean air; carcinoma of the thyroid gland), one animal of group 2 (brake dust low; carcinoma of the thyroid gland), in one animal of group 9 (amosite; carcinoma of the adrenal gland), and in one animal of group 9 (amosite; carcinoma of the liver). In one animal of group 4 (brake dust high) metastases from an organ outside the respiratory tract were detected, of which the origin remained unknown (primary site unknown) since no malignant tumor was seen on the slides provided. One animal of group 4 (brake dust high) showed an infiltration of the lung by lymphoma cells. The metastases and the lymphoma were interpreted to be incidental without any relation to the treatment.

4.3. Macroscopically suspected visceral pleural lesions in the lung

At necropsy, animals 8070, 8073, 8082, 8097, 9071, 9073, 9080, 9085, 9087, 9090, 9092, 9094, 9096, 9097, 9098, and 9171 (crocidolite: 8xxx and amosite: 9xxx, respectively) were observed to have macroscopic changes of the lung which were suspected to be visceral pleural lesions. Histopathological examination of these macroscopic lesions showed, however, that they correlated with bronchiolo-alveolar carcinoma, bronchiolo-alveolar adenoma or bronchiolo-alveolar hyperplasia (alveolar type with atypia) in the lung parenchyma. The lesions in the overlying lung visceral pleura consisted of (multi)focal very slight to slight mesothelial (visceral pleural) hyperplasias and/or pleural fibrosis. One animal, animal 9097 (amosite), showed an adhesion of the lung pleura to the thoracic wall. All of these pleural lesions were interpreted to be a consequence of the respective lung parenchymal lesions. Further, due to the mild extent (very slight to slight) of the pleural lesions, they were unlikely to have caused the macroscopically visible

Table 3
Neoplastic findings in the lung at the 2 year time point. 31 animals per group examined. Shown as well are the aerosol exposure concentrations of the number of fibers L > 20 μm/cm^3 and the total number of particles and fibers/cm^3.

Lung		Clean air control	Brake dust low	Brake dust mid	Brake dust high	Titanium-dioxide	Chrysotile low	Chrysotile high	Crocidolite	Amosite
# fibers (L > 20 μm)/cm^3		**0**	**0.2**	**0.4**	**0.5**	**0**	**28**	**72**	**24**	**48**
# Total Particles & fibers/cm^3		**117**	**506**	**589**	**793**	**2774**	**1279**	**1248**	**931**	**1185**
Number of animals examined		31	31	31	31	31	31	31	31	31
Malignant tumors	**Carcinoma, bronchiolo-alveolar**	0	0	0	1	1	0	0	3	3
	Adeno carcinoma	0	0	0	0	0	0	0	0	1
Benign tumors	**Adenoma, bronchiolo-alveolar with atypia**	0	0	0	0	0	0	0	1	1
	Adenoma, bronchiolo-alveolar	1	0	0	0	0	1	0	1	4
Total tumors		1	0	0	1	1	1	0	5*	9*

* $p < .05$ Chi-squared test (Campbell, 2007; Richardson, 2011)

Table 4
Bronchiole-alveolar hyperplasia in the lung at the 2 year time point. 31 animals per group examined. Shown for each type are the total number observed per group and grading of each lesion observed (from very slight to very severe).

Lung		Clean air control	Brake dust low	Brake dust mid	Brake dust high	Titanium-dioxide	Chrysotile low	Chrysotile high	Crocidolite	Amosite
# fibers (L > 20 μm)/cm^3		**0**	**0.2**	**0.4**	**0.5**	**0**	**28**	**72**	**24**	**48**
# Total Particles & fibers/cm^3		**117**	**506**	**589**	**793**	**2774**	**1279**	**1248**	**931**	**1185**
Number of animals examined		31	31	31	31	31	31	31	31	31
Hyperplasia	**Bronchiolo-alveolar, alveolar type with atypia**	**1**	**1**	**0**	**2**	**0**	**0**	**1**	**4**	**3**
	Very Slight	0	0	0	0	1	0	0	0	0
	Slight	0	0	0	0	0	0	0	0	0
	Moderate	0	0	0	0	0	0	0	3	0
	Severe	0	0	0	0	0	0	1	0	2
	Very severe	1	1	0	2	0	0	0	1	1
	Bronchiolo-alveolar, alveolar type	**1**	**5**	**1**	**4**	**3**	**4**	**7**	**8**	**6**
	Very Slight	0	3	0	1	1	1	1	2	1
	Slight	0	2	1	1	1	3	3	3	3
	Moderate	1	0	0	0	1	0	3	2	1
	Severe	0	0	0	1	0	0	0	1	1
	Very severe	0	0	0	1	0	0	0	0	0
	Bronchiolo-alveolar (bronchiolar type)	**0**	**0**	**2**	**4**	**3**	**6**	**20**	**30**	**30**
	Very Slight	0	0	2	3	3	3	18	4	3
	Slight	0	0	0	1	0	3	2	20	12
	Moderate	0	0	0	0	0	0	0	6	15
	Severe	0	0	0	0	0	0	0	0	0
	Very severe	0	0	0	0	0	0	0	0	0

changes alone.

4.4. Histopathological findings by exposure group

Key histopathological scores[3] are shown in Fig. 2 (45 d through 18 m) and Fig. 3 (24-month final sacrifice). The full histopathological report and findings are presented in the Sections S-2 and S-9, respectively (supplemental data). The Figs. 2 and 3 are presented separately as 4 rats/group were evaluated through 18 months and 31 rats/group scheduled for the final sacrifice (24 months)[4]. Representative histopathological images from each group at each time point are shown in Section S-3 (supplemental data). These results clearly differentiate the response following inhalation of brake dust as compared to chrysotile, crocidolite and amosite asbestos.

4.4.1. Air control group

The histopathological results in animals exposed to filtered air showed no exposure-related findings at any time point.

4.4.2. Brake dust exposed groups

In the brake dust groups at all time points, particle-laden macrophages (alveolar histiocytosis), predominantly at bronchiolo-alveolar junctions were observed in response to the inhaled particles. Particle-laden macrophages were also observed in the TiO_2 particle control group. At 180 days, in both the brake dust and TiO_2 groups, the incidences of very slight to slight (multi)focal accumulation of particle-laden macrophages in the bronchus-associated lymphoid tissue (BALT) were increased as compared to the previous sacrifices. From 6 months through 24 months a very slight dose dependent incidence continued to be observed. The BALT is part of the lymphatic system below the bronchial branching, which accumulate and likely transport particles cleared by the lymphatic system (Margaris and Black, 2012; Randall, 2010; Macklin, 1955; Semmler-Behnke et al., 2007). Interstitial fibrosis

[3] Grading scale for histopathology scoring: none (0), minimal (1), slight (2), mild (3), severe (4) and very severe (5). The numbers shown in Fig. 2 are the (histopathology score) X(the number of animals with that score), (e.g. 2 rats with slight (2) findings = 4). Fig. 3, final sacrifice, shows the total number with that finding.

[4] These animals were not necessarily sacrificed at the final timepoint, but due to their condition, preterminal euthanasia was also performed.

Color scale 1 2 3 4 5 6 7 8

Exposure group	Control						Brake dust low						Brake dust mid						Brake dust high						TiO2					
Time / Histopathological findings	45 d	90 d	3 m	6 m	12m	18m	45 d	90 d	3 m	6 m	12m	18m	45 d	90 d	3 m	6 m	12m	18m	45 d	90 d	3 m	6 m	12m	18m	45 d	90 d	3 m	6 m	12m	18m
Accumulation, Particle-Laden Macrophages, Alveolar/Interstitial	0	0	0	0	0	0	4	4	4	3	1	1	4	4	4	4	3	2	4	4	4	4	4	4	5	5	4	5	4	4
Accumulation, Fibre-Laden Macrophages, Alveolar/Interstitial	0	0	0	0	0	0	0	0	0	0	0	0	0	0	0	0	0	0	0	0	0	0	0	0	0	0	0	0	0	0
Fibrosis, Interstitial	0	0	0	0	0	0	0	0	1	0	0	0	0	0	0	0	0	0	0	0	0	0	0	0	0	0	0	0	0	0
Fibrosis, Pleural	0	0	0	0	0	0	0	0	1	0	0	0	0	0	0	0	0	0	0	0	0	0	0	0	0	0	1	0	0	0
Giant Cells, Syncytial	0	0	0	0	0	0	0	0	0	0	0	0	0	0	0	0	0	0	0	0	0	0	0	0	0	0	0	0	0	0
Hyperplasia, Bronchiolo-Alveolar	1	0	1	0	0	0	0	0	0	1	0	1	0	1	2	2	1	0	0	1	0	1	2	1	0	0	1	1	0	1
Hyperplasia, Bronchiolo-Alveolar; alveolar type with atypia, focal - Very Severe	0	0	0	0	0	0	0	0	0	0	0	0	0	0	0	0	0	0	0	0	0	0	0	0	0	0	0	0	0	0
Infiltration, Inflammatory Cell, Peribronchiolar	0	0	0	0	0	0	0	0	0	0	0	0	0	0	0	0	0	0	0	0	0	0	1	0	0	0	0	0	1	0
Infiltration, Inflammatory Cell, Perivascular	0	0	0	0	0	0	1	2	3	1	0	0	1	2	0	1	0	0	1	0	2	1	0	0	0	2	0	1	0	0
Infiltration, Inflammatory Cell, Pleural	0	0	0	0	0	0	0	0	0	0	0	0	0	0	1	0	0	0	0	0	0	0	0	0	0	0	0	0	0	0
Infiltration, Inflammatory Cell, Alveolar/Interstitial	0	0	0	0	0	0	0	0	0	0	0	0	0	0	0	0	0	0	0	0	0	0	0	0	0	1	0	2	0	1
Macrophage Aggregation, Alveolar	0	0	1	0	1	4	0	0	0	0	1	4	0	0	0	0	1	2	0	0	0	0	0	2	0	0	0	0	0	0
Microgranuloma	0	0	0	0	0	0	0	0	0	0	0	0	0	0	0	0	0	0	0	0	0	0	0	0	0	0	0	0	0	0
Accumulation, Particle-Laden Macrophages, Balt	0	0	0	0	0	0	0	0	2	1	2	0	0	0	3	1	4	1	0	0	2	3	3	3	1	0	4	3	4	4
Accumulation, Fibre-Laden Macrophages, Balt	0	0	0	0	0	0	0	0	0	0	0	0	0	0	0	0	0	0	0	0	0	0	0	0	0	0	0	0	0	0
Lung associated lymph nodes (LALN)						0						0						0						0						0
Accumulation, Particle-Laden Macrophages	0	0	0	0	0	0	1	0	3	1	0	0	1	1	3	3	3	0	1	1	3	4	4	0	1	1	2	4	5	0
Accumulation, Fibre-Laden Macrophages	0	0	0	0	0	0	0	0	0	0	0	0	0	0	0	0	0	2	0	0	0	0	0	4	0	0	0	0	0	4

Exposure group	Chrysotile low						Chrysotile high						Crocidolite						Amosite					
Time / Histopathological findings	45 d	90 d	3 m	6 m	12m	18m	45 d	90 d	3 m	6 m	12m	18m	45 d	90 d	3 m	6 m	12m	18m	45 d	90 d	3 m	6 m	12m	18m
Accumulation, Particle-Laden Macrophages, Alveolar/Interstitial	4	4	4	4	4	4	4	4	4	4	3	1	0	0	0	0	0	0	0	0	0	0	0	0
Accumulation, Fiber-Laden Macrophages, Alveolar/Interstitial	0	0	0	0	0	0	0	0	0	0	0	0	6	8	8	7	8	7	8	8	8	8	8	8
Fibrosis, Interstitial	0	0	0	1	1	0	0	2	4	4	1	0	4	5	8	6	7	7	4	8	8	8	9	8
Fibrosis, Pleural	2	0	0	0	0	0	0	0	1	0	0	0	1	0	1	0	0	0	1	1	2	3	0	0
Giant Cells, Syncytial	0	0	0	0	0	0	1	1	0	0	0	0	3	4	5	4	4	4	4	6	8	6	8	7
Hyperplasia, Bronchiolo-Alveolar	2	4	4	5	4	2	4	4	4	6	2	1	8	8	8	8	7	7	8	8	8	8	8	8
Hyperplasia, Bronchiolo-Alveolar; alveolar type with atypia, focal - Very Severe	0	0	0	0	0	0	0	0	0	0	0	0	0	0	0	0	0	5	0	0	0	0	0	5
Infiltration, Inflammatory Cell, Peribronchiolar	0	0	0	0	3	0	0	1	1	0	2	0	8	5	5	6	10	4	7	5	6	8	8	8
Infiltration, Inflammatory Cell, Perivascular	1	3	4	6	0	0	2	3	2	3	0	0	5	4	5	4	0	2	5	4	6	6	0	4
Infiltration, Inflammatory Cell, Pleural	0	0	0	0	0	0	0	0	1	0	0	0	0	0	0	0	0	0	1	0	0	0	0	0
Infiltration, Inflammatory Cell, Alveolar/Interstitial	0	3	2	4	0	1	0	4	4	4	0	0	5	8	8	6	0	4	8	8	8	8	0	8
Macrophage Aggregation, Alveolar	0	0	0	0	0	1	0	0	0	0	0	0	0	0	0	0	0	0	0	0	0	0	0	0
Microgranuloma	2	4	3	2	0	0	4	2	4	4	1	0	8	8	8	8	6	3	8	8	8	8	8	8
Accumulation, Particle-Laden Macrophages, Balt	1	0	4	4	2	1	0	0	4	4	3	1	0	0	0	0	0	0	0	0	0	0	0	0
Accumulation, Fibre-Laden Macrophages, Balt	0	0	0	0	0	0	0	0	0	0	0	0	0	1	4	4	2	3	0	1	4	4	3	3
Lung associated lymph nodes (LALN)						0						0						0						0
Accumulation, Particle-Laden Macrophages	1	2	4	1	0	0	0	0	3	3	3	0	0	0	0	0	0	5	0	0	0	0	0	7
Accumulation, Fibre-Laden Macrophages	0	0	0	0	0	0	0	0	0	0	0	0	0	3	6	6	6	0	1	2	4	6	5	0

Fig. 2. Summary of histopathological findings at 45, 89 days, 3, 6, 12, 18 months. Section S-9 (supplementary data) presents the individual results. The score shown is the product of the number of animals with the finding (from 0 to 4) and the grade for each animal (from 0 to 2) and ranged from 0 to 8. The grading system used for evaluation ranged as follows: 1) very slight/minimal, 2) slight, 3) moderate, 4) severe, 5) very severe. Eg: Group with 2 rats of score of 1 would be shown as 2. The colour scheme used in the table is shown above.

was not observed in any brake dust group over the course of the study.

4.4.3. TiO_2 exposed group

In the TiO_2 particle control group, particle-laden macrophages (alveolar histiocytosis), which were seen predominantly at the bronchiolo-alveolar junctions, were observed at all time points with severity ranging from very slight to slight.

4.4.4. Chrysotile exposed groups

Very slight (minimal) (multi)focal alveolar/interstitial accumulation of particle-laden macrophages (alveolar histiocytosis) were observed in the chrysotile exposed groups, predominantly at bronchiolo-alveolar junctions. These were found both during exposure and the post-exposure recovery period due to the considerable number of particles and shorter fibers present in the exposure aerosol. Multi-focal very slight microgranulomas (at bronchiolo-alveolar junctions) were observed in the low and high dose chrysotile groups (6 & 7) during exposure and during the post-exposure recovery period. Multi-focal interstitial fibrosis (very slight) was seen at 89 and 180 days in 2/4 rats of group 7 (chrysotile high). At 6 months postexposure, fibrosis (very slight) was seen in a single rat in group 6 and in all rats (very slight) in group 7. By 12 months post-exposure there was a single rat with interstitial fibrosis (very slight) in both groups 6 and 7. At both 18 and 24 months post exposure, interstitial fibrosis was not seen in group 6 (chrysotile low) and in group 7 (chrysotile high) only at 24 months, 1 rat out of 31 had very slight fibrosis.

4.4.5. Crocidolite and amosite exposure groups

At 45 days, accumulation of very slight (minimal) (multi) focal alveolar/interstitial fiber-laden macrophages (alveolar histiocytosis), was observed largely at the bronchiolo-alveolar junctions in the crocidolite and amosite exposure groups (Grps 8 & 9). This was accompanied as well by multifocal peribronchial/peribronchiolar and alveolar/interstitial (intraseptal) infiltration of (mixed) inflammatory cells with slight multi-focal microgranulomas at the bronchiolo-alveolar junctions. Very slight multi-focal interstitial fibrosis was observed in all rats at each time point through 180 days. By 6 months post-exposure, this had increased to very slight to slight interstitial fibrosis in the crocidolite animals and slight interstitial fibrosis in the amosite animals. In addition, 2/4 males of group 9 (amosite) showed very slight or slight focal pleural fibrosis. Similar findings were observed at 12, 18 and 24 months post-exposure.

4.5. Wagner grading system

The Wagner grades are shown in Figs. 4 and 5. The Wagner grading system clearly differentiates between grade 3 and grades 4–8. Through grade 3 represents "cellular change" (inflammatory and reversible) while grade 4 and above represents progressive degrees of fibrosis which may not be totally reversible (McConnell and Davis, 2002)[5]. The interpretation of the range of findings included in Wagner grade 4 is presented in the discussion below.

Brake dust groups: Wagner grades 1 and 2 occurred at all time points

[5] Grade 1 = No lesion observed.Grade 2 = A few macrophages in the lumen of the terminal bronchioles and alveoli.Grade 3 = Presence of cuboidal epithelium lining the proximal alveoli (bronchiolization). No collagen but reticulin fibres may be present in the interstitium at the junction of the terminal bronchiole and alveolus. Luminal macrophages are more conspicuous and mononuclear cells may be found in the interstitium.Grade 4 = Minimal collagen deposition at the level of the terminal bronchiole and alveolus. Increased bronchiolization with associated mucoid debris suggesting glandular pattern (see Methods section for details on Grade 4).Grade 5 = Interlobular linking of the lesions described in Grade 4 and increased severity of fibrosis.Grade 6 = Early consolidation. Parenchymal decrease is apparent.Grade 7 = Marked fibrosis and consolidation.Grade 8 = Complete obstruction of most airways.

Color scale	0	1-4	5-9	10-14	15-19	20-24	25-29	30	31

Final Sacrifice	Clean air control	Brake dust low	Brake dust mid	Brake dust high	Titanium-dioxide	Chrysotile low	Chrysotile high	Crocidolite	Amosite
Histopathological Findings									
LUNG									
Examined	31	31	31	31	31	31	31	31	31
Adenocarcinoma; malignant	0	0	0	0	0	0	0	0	1
Adenoma, Bronchiolo-Alveolar; benign	1	0	0	0	0	1	0	1	4
Adenoma, Bronchiolo-Alveolar; with atypia, benign	0	0	0	0	1	0	0	1	1
Carcinoma, Bronchiolo-Alveolar; malignant	0	0	0	1	0	0	0	3	3
alveolar/interstitial; Accumulation, Fibre-Laden Macrophages; multifocal	**0**	**0**	**0**	**0**	**0**	**0**	**0**	**29**	**29**
very slight	0	0	0	0	0	0	0	21	18
slight	0	0	0	0	0	0	0	8	11
alveolar/interstitial; Accumulation, Particle-Laden Macrophages; multifocal	**0**	**3**	**10**	**22**	**25**	**19**	**22**	**0**	**0**
very slight	0	3	10	20	24	19	22	0	0
slight	0	0	0	2	1	0	0	0	0
interstitial; Fibrosis; focal	**0**	**0**	**0**	**0**	**0**	**0**	**1**	**0**	**0**
very slight	0	0	0	0	0	0	1	0	0
interstitial; Fibrosis; multifocal	**0**	**0**	**0**	**0**	**0**	**0**	**0**	**29**	**29**
very slight	0	0	0	0	0	0	0	16	9
slight	0	0	0	0	0	0	0	13	20
pleural; Fibrosis; focal	**1**	**0**	**0**	**0**	**0**	**0**	**0**	**1**	**1**
very slight	1	0	0	0	0	0	0	1	0
slight	0	0	0	0	0	0	0	0	1
pleural; Fibrosis; multifocal	**1**	**0**	**0**	**0**	**0**	**0**	**0**	**0**	**0**
very slight	1	0	0	0	0	0	0	0	0
Giant Cells, Syncytial; multifocal	0	0	0	0	0	0	0	26	27
very slight	0	0	0	0	0	0	0	26	27
Hyperplasia, Bronchiolo-Alveolar; multifocal	**0**	**0**	**1**	**1**	**0**	**3**	**15**	**30**	**30**
very slight	0	0	1	1	0	3	13	4	3
slight	0	0	0	0	0	0	2	20	12
moderate	0	0	0	0	0	0	0	6	15
Hyperplasia, Bronchiolo-Alveolar; alveolar type, focal	**1**	**5**	**1**	**4**	**2**	**4**	**5**	**7**	**6**
very slight	0	3	0	1	0	0	1	2	1
slight	0	2	1	1	1	3	2	3	3
moderate	1	0	0	0	1	1	2	1	1
severe	0	0	0	1	0	0	0	1	1
very severe	0	0	0	1	0	0	0	0	0
peribronchiolar; Infiltration, Inflammatory Cell; multifocal	**0**	**0**	**0**	**0**	**0**	**0**	**0**	**10**	**11**
very slight	0	0	0	0	0	0	0	10	10
slight	0	0	0	0	0	0	0	0	1
perivascular; Infiltration, Inflammatory Cell; multifocal	**0**	**0**	**0**	**0**	**0**	**0**	**0**	**10**	**12**
very slight	0	0	0	0	0	0	0	10	12
alveolar/interstitial; Infiltration, Inflammatory Cell; multifocal	**0**	**0**	**0**	**0**	**1**	**1**	**1**	**27**	**28**
very slight	0	0	0	0	1	1	0	24	24
slight	0	0	0	0	0	0	1	3	4
Inflammation, Chronic; multifocal	**11**	**5**	**11**	**3**	**4**	**10**	**10**	**1**	**3**
very slight	5	4	8	2	3	9	8	0	3
slight	6	1	3	1	1	1	2	1	0
Macrophage Aggregation, Alveolar; multifocal	**22**	**18**	**20**	**21**	**16**	**20**	**18**	**9**	**10**
very slight	12	10	12	12	15	7	8	6	3
slight	9	7	6	9	1	12	10	3	7
moderate	1	1	2	0	0	1	0	0	0
Microgranuloma; multifocal	**0**	**0**	**0**	**0**	**0**	**0**	**0**	**21**	**24**
very slight	0	0	0	0	0	0	0	21	24
Accumulation, Particle-Laden Macrophages, Balt; focal	**0**	**0**	**1**	**0**	**1**	**1**	**0**	**0**	**0**
very slight	0	0	1	0	1	1	0	0	0
Accumulation, Particle-Laden Macrophages, Balt; multifocal	**0**	**0**	**0**	**6**	**19**	**0**	**2**	**0**	**0**
very slight	0	0	0	6	19	0	2	0	0
Accumulation, Fibre-Laden Macrophages, Balt; multifocal	**0**	**0**	**0**	**0**	**0**	**0**	**0**	**4**	**5**
very slight	0	0	0	0	0	0	0	4	5

Final Sacrifice	Clean air control	Brake dust low	Brake dust mid	Brake dust high	Titanium-dioxide	Chrysotile low	Chrysotile high	Crocidolite	Amosite
Histopathological Findings									
LUNG ASSOCIATED LYMPH NODES (laln)									
Examined	28	29	26	30	30	28	28	29	30
No Visible Lesions	27	28	24	22	11	22	19	11	17
Not Examined: No Significant Tissue Present In Section	3	2	5	1	1	3	2	2	1
Not Examined: Tissue Not Taken At Necropsy	0	0	0	0	0	0	1	0	0
Accumulation, Fibre-Laden Macrophages; multifocal	**0**	**0**	**0**	**0**	**0**	**0**	**0**	**16**	**11**
very slight	0	0	0	0	0	0	0	8	11
slight	0	0	0	0	0	0	0	8	0
Accumulation, Particle-Laden Macrophages; focal	**0**	**0**	**0**	**0**	**2**	**1**	**1**	**0**	**0**
very slight	0	0	0	0	2	1	1	0	0
Accumulation, Particle-Laden Macrophages; multifocal	**0**	**0**	**2**	**6**	**16**	**2**	**5**	**0**	**0**
very slight	0	0	2	6	14	2	5	0	0
slight	0	0	0	0	2	0	0	0	0

Fig. 3. Summary of histopathological findings at 24 months. Section S-9 (supplementary data) presents the individual results. The score shown is the number of animals with the finding (from 0 to 31) for each grade. The grading system used for evaluation ranged as follows: 1) very slight/minimal, 2) slight, 3) moderate, 4) severe, 5) very severe. The colour scheme used in the table is shown above.

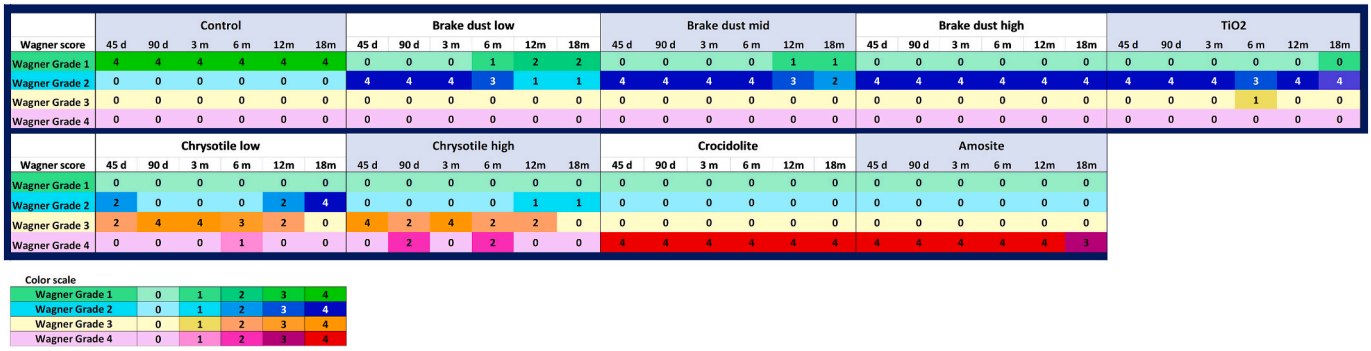

	Control						Brake dust low						Brake dust mid						Brake dust high						TiO2					
Wagner score	45 d	90 d	3 m	6 m	12m	18m	45 d	90 d	3 m	6 m	12m	18m	45 d	90 d	3 m	6 m	12m	18m	45 d	90 d	3 m	6 m	12m	18m	45 d	90 d	3 m	6 m	12m	18m
Wagner Grade 1	4	4	4	4	4	4	0	0	0	1	2	2	0	0	0	0	1	1	0	0	0	0	0	0	0	0	0	0	0	0
Wagner Grade 2	0	0	0	0	0	0	4	4	4	3	1	1	4	4	4	4	3	2	4	4	4	4	4	4	4	4	4	3	4	4
Wagner Grade 3	0	0	0	0	0	0	0	0	0	0	0	0	0	0	0	0	0	0	0	0	0	0	0	0	0	0	0	1	0	0
Wagner Grade 4	0	0	0	0	0	0	0	0	0	0	0	0	0	0	0	0	0	0	0	0	0	0	0	0	0	0	0	0	0	0

	Chrysotile low						Chrysotile high						Crocidolite						Amosite					
Wagner score	45 d	90 d	3 m	6 m	12m	18m	45 d	90 d	3 m	6 m	12m	18m	45 d	90 d	3 m	6 m	12m	18m	45 d	90 d	3 m	6 m	12m	18m
Wagner Grade 1	0	0	0	0	0	0	0	0	0	0	0	0	0	0	0	0	0	0	0	0	0	0	0	0
Wagner Grade 2	2	0	0	0	2	4	0	0	0	0	1	1	0	0	0	0	0	0	0	0	0	0	0	0
Wagner Grade 3	2	4	4	3	2	0	4	2	4	2	2	0	0	0	0	0	0	0	0	0	0	0	0	0
Wagner Grade 4	0	0	0	1	0	0	0	2	0	2	0	0	4	4	4	4	4	4	4	4	4	4	4	3

Color scale					
Wagner Grade 1	0	1	2	3	4
Wagner Grade 2	0	1	2	3	4
Wagner Grade 3	0	1	2	3	4
Wagner Grade 4	0	1	2	3	4

Fig. 4. Wagner scores at 45, 89 days, 6, 12, 18 monthsfor each group. The number shown is the number of animals for each group/time point (maximum 4) with that Wagner score. The color scale is shown below.

LUNG	Clean air control	Brake dust low	Brake dust mid	Brake dust high	Titanium-dioxide	Chrysotile low	Chrysotile high	Crocidolite	Amosite
Examined	31	31	31	31	31	31	31	31	31
Wagner Grade 1	31	28	21	9	6	12	4	0	0
Wagner Grade 2	0	3	10	22	25	18	14	0	0
Wagner Grade 3	0	0	0	0	0	1	12	0	0
Wagner Grade 4	0	0	0	0	0	0	1	31	31

Color scale Grade 1	0	1-6	7-12	13-18	19-25	26-31
Color scale Grade 2	0	1-6	7-12	13-18	19-25	26-31
Color scale Grade 3	0	1-6	7-12	13-18	19-25	26-31
Color scale Grade 4	0	1-6	7-12	13-18	19-25	26-31

Fig. 5. Wagner scores at 24 months for each group. The number shown is the number of animals for each group/time point (maximum 31) with that Wagner score. The color scale is shown below.

which reflects the normal clearance by macrophages of the particles.

Chrysotile low dose group: Grades 2 and 3 were observed through 18 month reflecting the increased cellular activity in response to the higher particle and fiber exposure with a single animal showing very slight fibrosis at 6 months. By 24 months, out of 31 animals, 12 had grade 1, 18 grade 2 and 1 grade 3.

Chrysotile high dose group: Primarily grade 3 was observed through 12 months post-exposure with 2 animals at 90 day and 6 months showing very slight fibrosis grade 4. At 18 months, 1 animal sacrificed showed grade 2. At 24 months, out of 31 animals, 4 had grade 1, 14 grade 2, 12 grade 3 and 1 grade 4.

Crocidolite and amosite groups: At all time points from 45 days through 24 months, grade 4 was observed (Figs. 4 and 5). This corresponds to the persistence of the biopersistent long crocidolite and amosite fibers in the lung, which appear to continuously stimulate the inflammatory response of the lung producing sustained fibrosis. Shorter fibers that are trapped in the inflammatory lesions also persist.

4.6. McConnell & Davis fibrosis quantification

As explained above, as a more quantitative indicator of fibrotic response among those animals that were graded 4 under the Wagner system (see above), the total area of the lung showing fibrosis was quantified by Fraunhofer on the histopathological slides of the lung from 45 days through 18 months using the method of McConnell and Davis (2002). Fibrosis was observed in the chrysotile low dose group at 6 months in a mean of 0.08 % of the histopathological slide examined. In the chrysotile high dose, fibrosis was observed at 89 days in a mean of 0.28 % of the histopathological slides and at 6 months 0.27 % (Table 6).

In the crocidolite exposed animals, the percent fibrosis started at 0.43 % at 45 days, increased to 0.75 % at 89 days and then further increased to between 0.96 and 1.07 % through 18 months. In the amosite exposed animals, the percent fibrosis started at 0.77 % at 45 days, and then also further increased to between 0.99 and 1.10 % through 18 months.

5. Confocal microscopy

5.1. Confocal microscopy: pathological response in the lung

Through the use of multiplexed confocal microscopy, the temporal and spatial distribution of each test article in the lung and the associated inflammatory responses was assessed. In the lung parenchyma, the amount of collagen present in the connective tissue was quantified at 45 days, 89 days (end of exposure), 3, 6, 12, 18 and 24 months. The percent collagen at 45 days, 89 days (end of exposure) and at 3 months (90 days post exposure) have been presented previously (Bernstein et al., 2019b). Fig. 6 shows the subsequent analyses of the percent collagen in the lung at 6, 12, 18 and 24 months.

As was reported earlier for the first three time-points (Bernstein et al., 2019b), through 24 months, there were no statistically significant differences in the percent collagen in the lungs as compared to the controls for the brake dust groups, the TiO_2 group or the chrysotile groups.

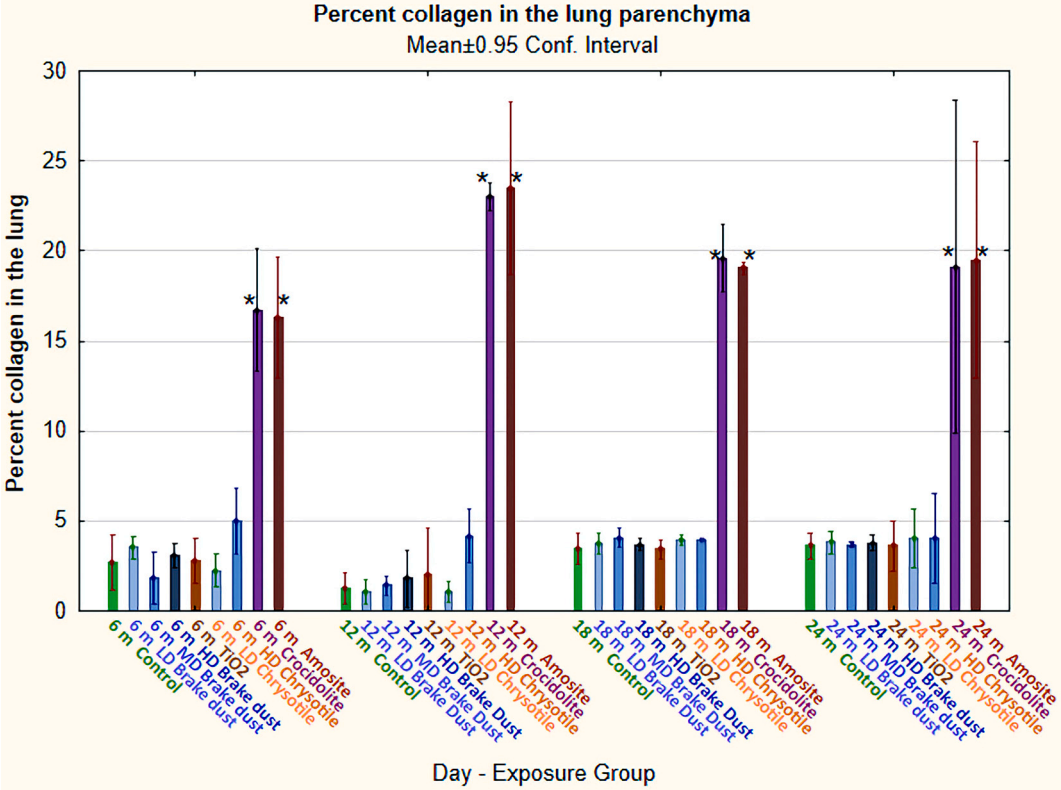

Fig. 6. Confocal microscopy – Lung Parenchyma Percent Collagen at 6, 12, 18 and 24 m (Percent collagen = volume of the parenchyma collagen/volume of parenchyma tissue×100) shown by group and day (Means ± SE). * Dunnett's test $p < .0001$ as compared to the control.

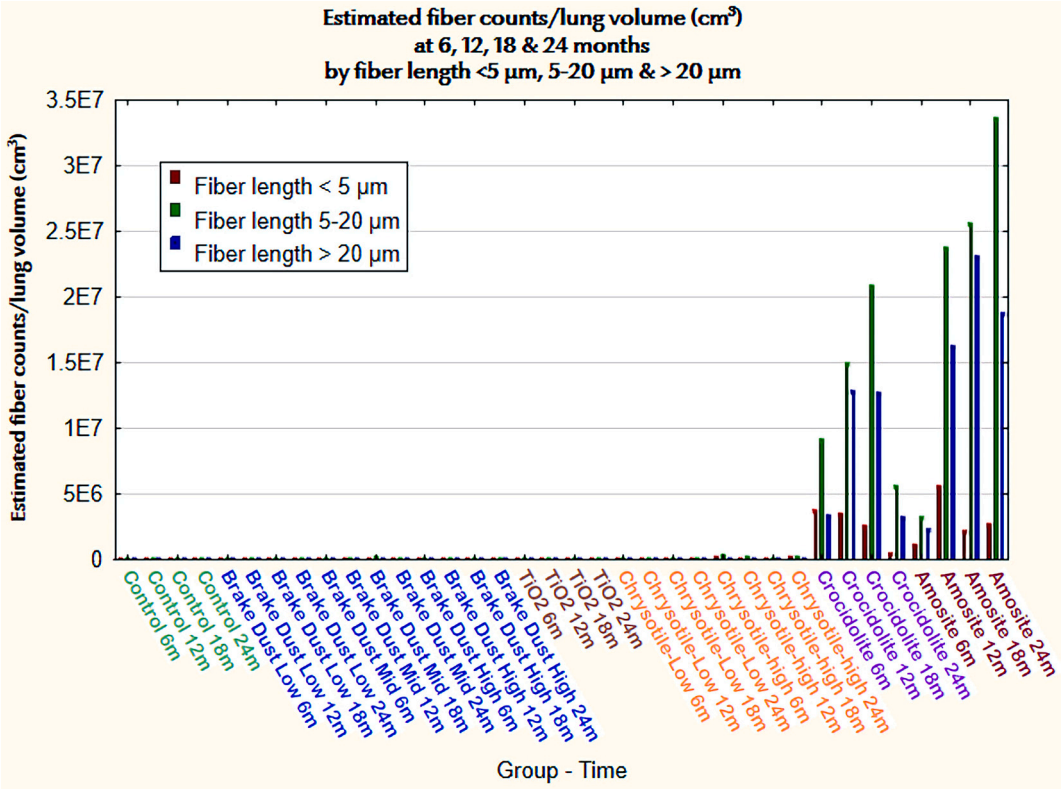

Fig. 7. Confocal analysis of the number and length of fibers (< 5 µm 5–20 µm & > 20 µm) in the lung parenchyma at 6, 12, 18 and 24 m.

In both the crocidolite and amosite groups at 6, 12, 18 and 24 months, the mean percent collagen in the lung remained increased compared to the controls at each time point ($p < .0001$) (similar to as was reported earlier at 45, 89 d and 3 m, Bernstein et al., 2019b). For both crocidolite and amosite the increase over this time ranged from 14 to 23% as compared to the means of the control groups at each time point.

The one-way ANOVA analysis and Dunnett's tests are presented in Section S-4 (Supplementary data).

Confocal analysis also allowed the measurement of the length of fibers observed in both the airways and the parenchyma. From the number of fibers/tissue volume the total lung parenchyma concentration of fibers per cm^3 of lung tissue was estimated assuming an even distribution (Fig. 7).

In the large conducting airways in all groups, few if any fibers were observed. In the air control and TiO_2 groups, the fibrous-shaped objects observed in the parenchyma were not chrysotile. In the brake dust groups and in the chrysotile exposed groups, the few fibers observed in the parenchyma had lengths in the range of < 5 to 20 μm with no fibers > 20 μm. In the crocidolite and amosite exposed groups, considerably greater numbers of fibers were found in the parenchyma in each size category and only in these two groups were fibers longer than 20 μm found.

5.1.1. Confocal microscopy images of the lung

In each group, confocal images of the lungs at 6, 12, 18 and 24 months were taken with the same procedures as reported earlier for 45, 89 and 180 days (Bernstein et al., 2019b). This procedure preserved the spatial and cellular orientation of particles and fibers in the lung. Using serial section stacks of image data and 3D projection images, maximum intensity projections of fields of view in the lung airways and parenchyma were recorded for each group.

Confocal images of the lung for each group at 6, 12, 18 and 24 months are presented in the Sections S-4.1–S-4.4 of the Supplemental data[6]. Very little difference is observed in the brake dust exposed groups (2–4) compared to the air controls (Grp 1). In the high dose brake dust (Grp 4) a slight increase in the number of macrophages can be noted, which is a normal response to the particles present in the brake dust. In the TiO_2 Grp 5, macrophages are seen with numerous TiO_2 particles at all time points. The low dose chrysotile (Grp 6) appears as well very similar to the air control group. In the high dose chrysotile (Grp 7) occasional fibers are observed. The groups exposed to amphibole asbestos (8 and 9) show a distinctively different response at all time points. Numerous fibers, both long and short, including fibers longer than 40 μm, with alveolar macrophages and granulomas, are present. This is accompanied by an extensive collagen matrix that persists through 24 months.

Fig. 8, plates 1-4, show representative images[8] in greater detail from the air control, high dose brake dust, high dose chrysotile and amosite groups (Grps 1, 4, 7 and 9) at 24 months. The brake dust exposed high dose looks very similar to the air control also with occasional macrophages. In the chrysotile high dose group at 24 months, macrophages are seen in the alveoli with occasional short chrysotile fibers.

Through 24 months in groups 2–7 the response to the exposures diminishes. This is in contrast to the amphibole groups 8 & 9 where the collagen matrix continues to develop in response to the persistent presence of longer and shorter fibers.

Fig. 8, Panel 4 shows the response to amosite asbestos at 24 months. A localized collagen response in the interstitial connective tissue occurs in response to the amosite fibers, which can be seen penetrating and traversing the airway wall. The numerous long amosite fibers are often associated with granuloma and intense collagen response.

5.2. Pathological response in the pleural cavity – confocal microscopy

In the visceral and parietal pleural, the percent collagen as determined by confocal microscopy in the connective tissue at 9, 12, and 18 months are shown in Figs. 9 and 10. In addition, the mesothelial thickness of the visceral and parietal pleura is shown in Figs. 11 and 12. No animals were allocated at 24 months for the deep-frozen pleural cavity analysis in order to prioritize the histopathology examination at 24 months. Similar analysis was reported for the earlier time points at 45, 89 d and 3 m (Bernstein et al., 2019b).

For the brake dust, TiO_2 or chrysotile exposed animals, no statistically significant differences compared to the controls were observed in either the visceral or parietal pleural percent collagen or mesothelial thickness. Through 18 months, for both the crocidolite and the amosite exposed groups, the percent collagen and mesothelial thickness of the visceral and parietal pleural as compared to the control group were significantly increased ($p < .0001$, ANOVA/Dunnett's test).

For crocidolite the mean differences in percent collagen with the control were similar over 9, 12 and 18 months and ranged from 13 to 19 % in the visceral pleura and 12–17 % in the parietal pleura. For amosite, the mean differences over 9, 12, and 18 months with the control group were 13–17 % in the visceral pleura and 12–17 % in the parietal pleura. The statistical comparison of the percent collagen by group and time point is presented in Section S-5 (Supplemental data).

Concurrent with the collagen formation in the amphibole asbestos-exposed groups was the statistically significant increase in mesothelial layer thickness of both the visceral and parietal pleural as compared to the control groups ($p < .0001$, ANOVA/Dunnett's test) (Figs. 11 and 12). The mean visceral mesothelial thickness of the control group ranged from 4.5 to 4.7 μm while that of the amphibole exposed groups ranged from 11.6 to 19.2 μm. The mean parietal mesothelial thickness of the control group ranged from 2.7 to 5.0 μm while that of the amphibole exposed groups ranged from 18.9 to 30.8 μm. There were no statistically significant differences from control in mesothelial thickness in any of the brake dust, TiO_2, or chrysotile exposed groups. The statistical comparison of the mesothelial thickness between groups and time points is presented in Section S-7 (Supplemental data).

Confocal images of the chest walls, including visceral and parietal pleura from animals in each group at 9, 12, and 18 months were taken using confocal microscopy (with the same procedures as reported earlier for 45, 89, and 180 days (Bernstein et al., 2019b)). This procedure preserved the spatial and cellular orientation of particles and fibers in the tissue. Using serial section stacks of image data and 3D projection images, maximum intensity projections of fields of the chest walls, including visceral and parietal pleura, were collected. There was occasional minor contraction of the lung during the freezing process, which sometimes produced a wavy orientation of the visceral pleural surface.

Representative images of the parietal and visceral pleura in each group at 9, 12, and 18 months are shown in Section S-6 (Supplemental data). The images are colored as follows: Sub-pleural alveolar septa and pleural space cells are shown in shades of green. The visceral and (when present) parietal pleura surfaces which are high in collagen content, are shown in bright green linear profiles. Shown in orange are particles and or fibers (if present) in conjunction with lung or pleura tissue.

Fig. 13 shows in 3D, details of the responses in the visceral and parietal pleura from the air control, high dose brake dust, high dose chrysotile, crocidolite, and amosite groups (1, 4, 7, 8 & 9) at 18 months.

An air control animal is shown in Fig. 13, Plate 1. This image provides extensive detail of the structure and drainage of the pleural pathways from the chestwall/parietal pleura (Bernstein and Pavlisko, 2017; Negrini and Moriondo, 2013). The accumulation space behind a lymphatic stomata can be seen. This leads into large sub-mesothelial lymphatics through uni-directional secondary valves, which insure that the fluid flow is away from the parietal pleura. The lower sub-

[6] Connective tissue cables are shown in bright green from maximum intensity projections of the original images. In orange are the particles and fibers and if they are protein coated appear yellow.

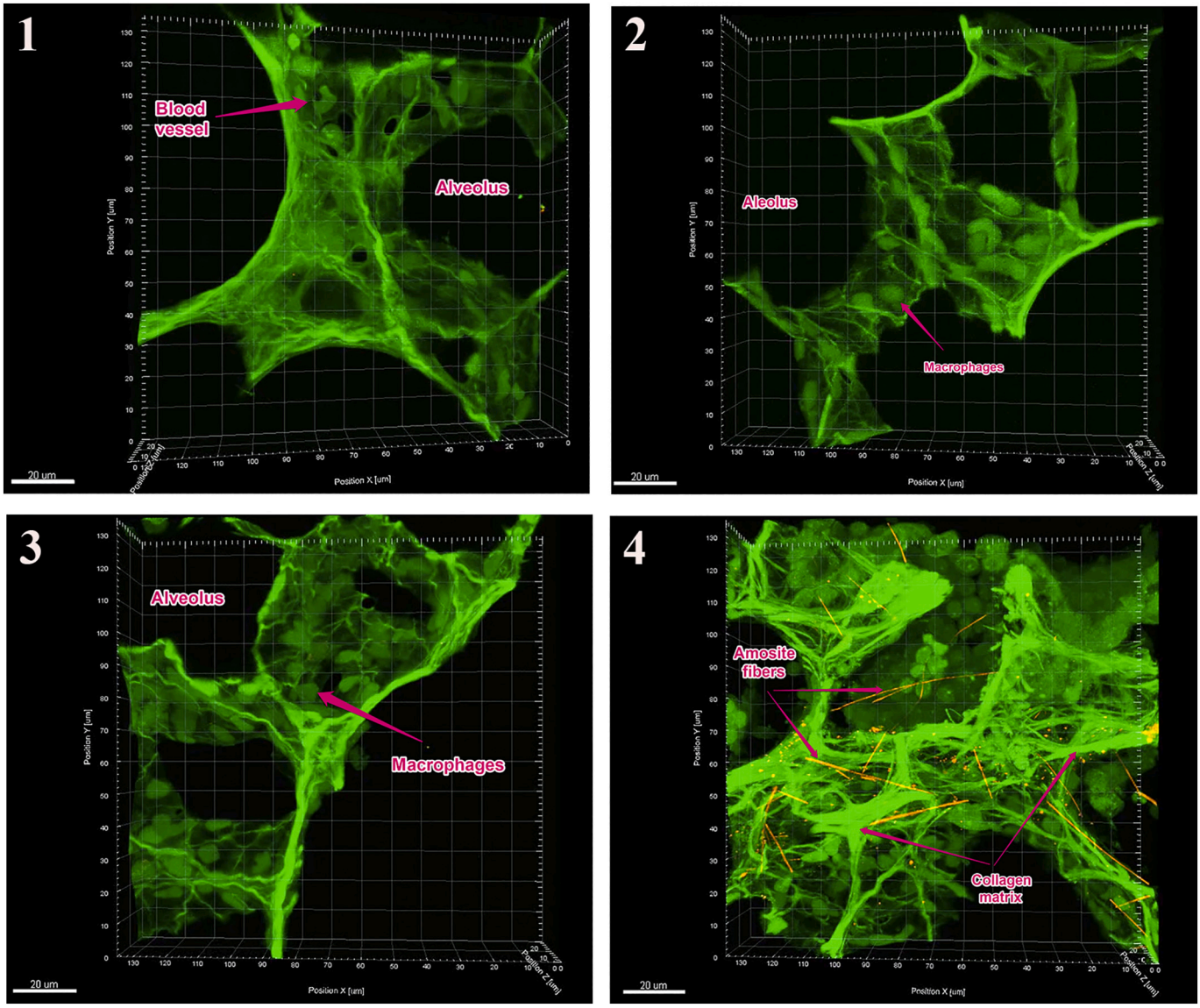

Fig. 8. Representative confocal images of the lung in groups 1, 4, 7 and 9 at 24 months[8]. Scale bars in μm are included for each image.
Panel 1: Group 1, air control: Normal parenchyma with macrophages in alveoli and a blood vessel
Panel 2: Group 2, brake dust high dose: Normal parenchyma with macrophages in alveoli.
Panel 3: Group 7, chrysotile high dose. Normal parenchyma, alveoli with macrophages in alveoli.
Panel 4: Group 9, amosite: Numerous long and shorter amosite fibers are observed in the lung parenchyma with an extensive collagen matrix and alveolar macrophages and granulomas.

mesothelial lymphatic channel can be seen draining into a deep lymphatic collector.

Plate 2 shows the visceral and parietal pleura in the high dose brake dust (Grp. 4), which appears similar to the air control. A brake dust particle is seen in the lung without any inflammatory response. Plate 3 shows a similar image for the high dose chrysotile group with no inflammatory response.

The amphibole asbestos-exposed groups are in marked contrast as shown in plates 4–6. Plate 4 shows a crocidolite exposed animal at 18 months. Long crocidolite fibers are seen in the lung and penetrating into and through the visceral pleura. Collagen development is seen within the lung and especially in a thickened visceral pleura (the parietal pleura was not captured in this view). Plates 5 and 6 show an amosite exposed animal. In Plate 5, a long amosite fiber is seen in the pleural space with a pleural adhesion joining the visceral and parietal surfaces. The lung shows extensive inflammation as well. In Plate 6, again with amosite asbestos, another adhesion is seen with extensive collagen development on both the visceral and parietal pleura.

6. Discussion

This repeated-dose 90-day inhalation toxicology study with life-time follow-up (through ~20 % survival at ~24 months) demonstrates clearly that brake dust from brakes that used chrysotile in the matrix, resulted in no inflammatory response or exposure-related tumors at exposure concentrations and deposited doses, which were orders of magnitude greater than those reported for worker exposure (Bernstein et al., 2019a).

This long-term inhalation toxicology study of brake dust with control groups of TiO_2, chrysotile, and the amphibole asbestos crocidolite and amosite, is the first to be performed at exposure concentrations within a few orders of magnitude of past human exposures. Comparable exposures were assured for the chrysotile and amphibole asbestos groups in this study by producing fiber aerosols with similar long fiber (> 20 μm)

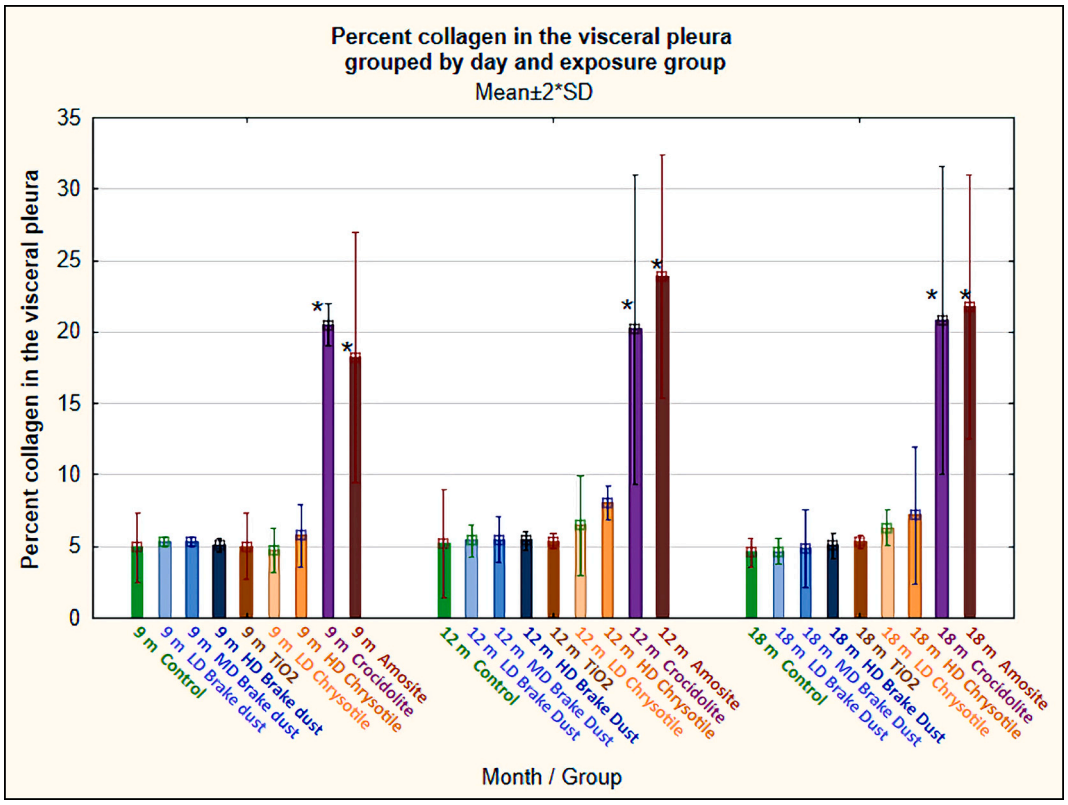

Fig. 9. Confocal microscopy quantification of the percent collagen in the visceral pleura at 9, 12 and 18 m (Percent collagen = volume of collagen/volume of visceral pleural tissue×100) shown by group and day (Means ± SD). * ANOVA/Dunnett's test $p < .0001$ as compared to the control

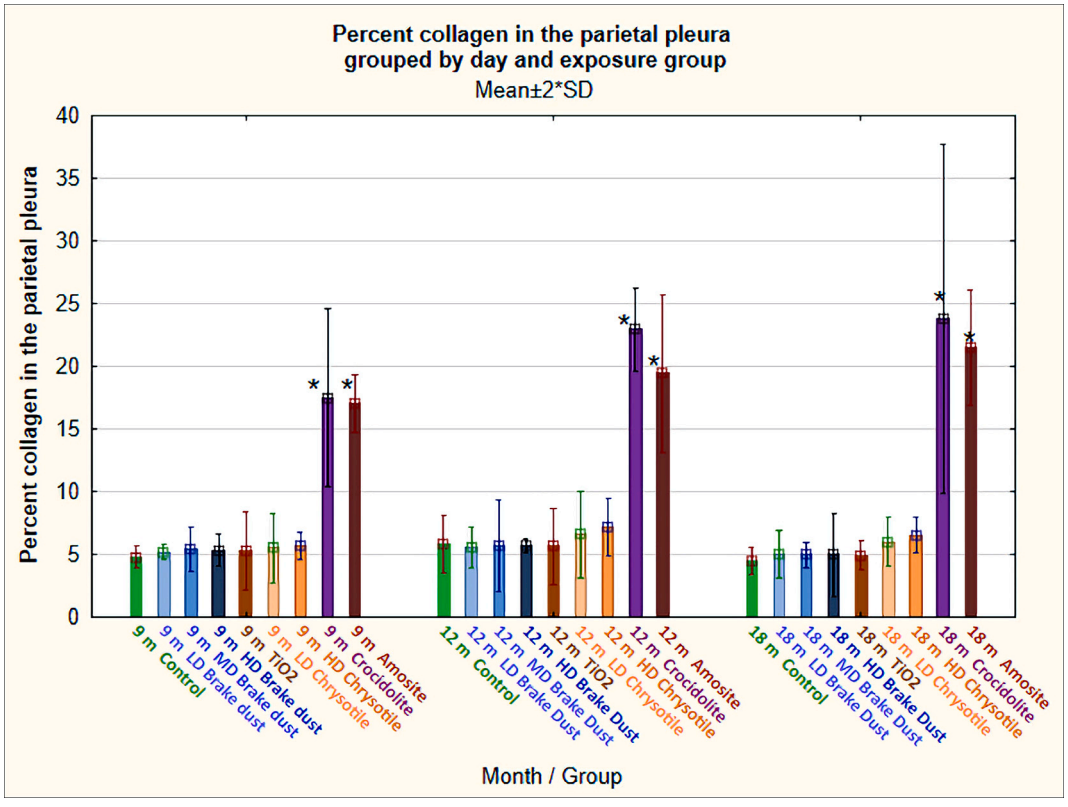

Fig. 10. Confocal microscopy quantification of the percent collagen in the parietal pleura at 9, 12 and 18 m (Percent collagen = volume of collagen/volume of visceral pleural tissue×100) shown by group and day (Means ± SD). * ANOVA/Dunnett's test $p < .0001$ as compared to the control.

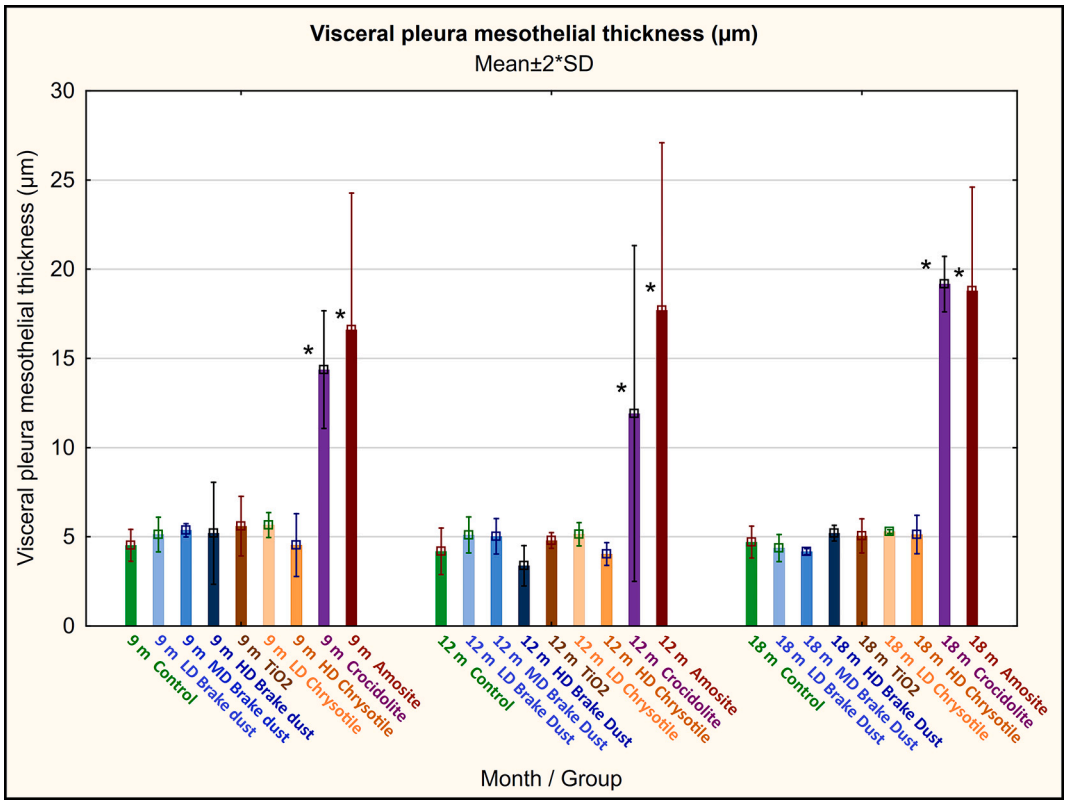

Fig. 11. Confocal microscopy quantification of the visceral pleura mesothelial thickness (µm) at 9, 12 and 18 m. * ANOVA/Dunnett's test $p < .0001$ as compared to the control.

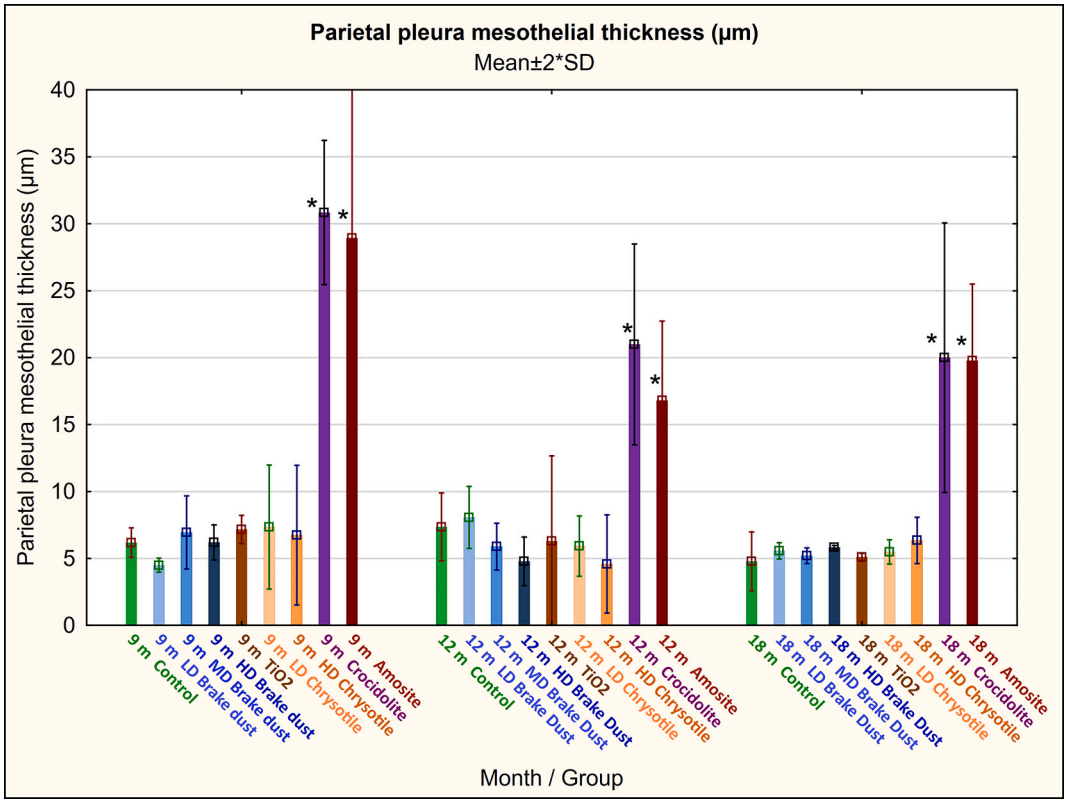

Fig. 12. Confocal microscopy quantification of the parietal pleura mesothelial thickness (µm) at 9, 12 and 18 m. * ANOVA/Dunnett's test $p < .0001$ as compared to the control.

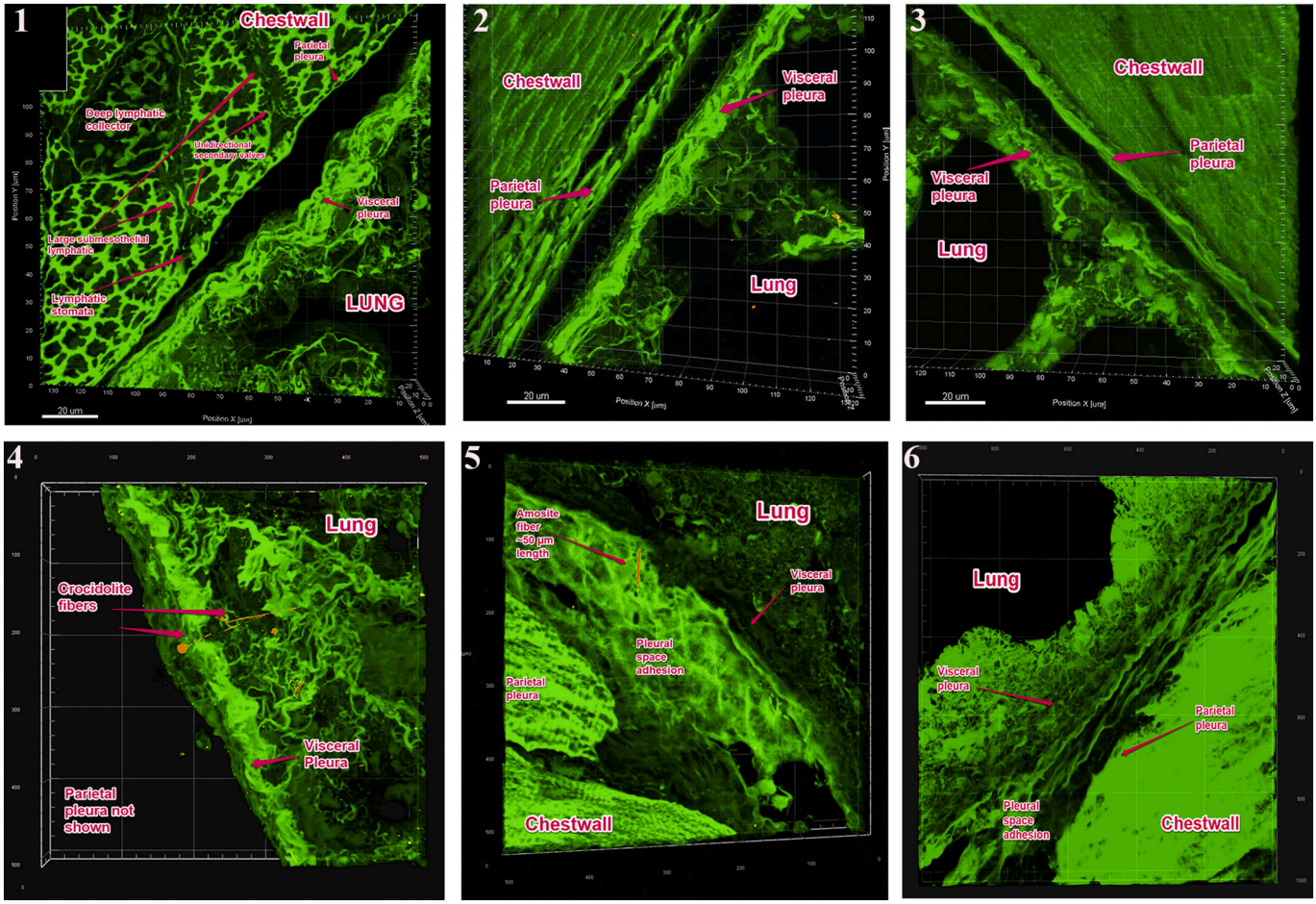

Fig. 13. Representative confocal images of the pleural cavity for groups 1, 4, 7, 8 & 9 at 18 months. Bright green structures are connective tissue cables highlighted using maximum intensity projection from original image data. Particles and fibers are shown in orange. When protein coated they appear yellow. These images are from projected three dimensional reconstructions. The scale bars are in µm and are shown in each image in the surrounding frames.
Panel 1: Group 1, Air control Pleura: Shown are the visceral and parietal pleura. The parietal pleura shows lymphatic stomata, unidirectional secondary valves, large submesoithlial lymphatics and a deep lymphatic colletor.
Panel 2: Group 4 High dose brake dust Pleura: Shown are the visceral and parietal pleura which appear similar to that of the air control.
Panel 3: Group 7 Chrysotile high dose Pleura: Shown are the visceral and parietal pleura which appear similar to that of the air control.
Panel 4: Group 8 Crocidolite asbestos Pleura: Shown is only the visceral pleura (the parietal pleura was out of the view). Long crocidolite fibers can be seen in the subpleural alveoli and extending into the pleural cavity. An extensive collagen matrix surrounds the area.
Panel 5: Group 9 Amosite asbestos Pleura: Shown are the visceral and parietal pleura joined by a pleural adhesion and with an amosite fiber embedded in the adhesion.
Panel 6: Group 9 Amosite asbestos Pleura: Shown are the visceral and parietal pleura joined by a pleural adhesion.

concentrations. Equally important, the aerosol was generated without extensively milling or grinding the fibers, thereby allowing a direct comparison between fiber types as presented earlier (Bernstein et al., 2019a).

The power of this study was further enhanced by using two independent methods for assessment of the pathological endpoints, histopathological examination, and quantitative confocal microscopy. This further facilitated assessment of possible mechanisms by which fibers may or may not translocate to the pleural cavity and produce disease.

The brake dust in this study was obtained from grinding automobile brakes that were produced using chrysotile in the formulation matrix (Bernstein et al., 2018). Such brakes typically contained between 30 and 70% asbestos (Bernstein et al., 2018; Blau, 2001). In this study, the brake dust aerosols contained a mean of 1297–2120 fibers(total)/cm^3. Of these, there were only between 2 and 7 WHO fibers/cm^3 (means). Fewer fibers L > 20 µm were in the aerosol (means 0.2- 0.5 fibers L > 20 µm)/cm^3). Brake drums, when wearing, appear to favor the production of very short (< 5 µm) chrysotile fibers (Blau, 2001; Rhee, 1974). Assuming 30% chrysotile in the brake pads, from the chrysotile gravimetric and WHO fiber concentration, the WHO fibers in the brake dust aerosol account for < 2% of the total aerosol mass.

The TiO_2 particle control was exposed using a gravimetric concentration equivalent to that of the high dose brake dust group (0.67 vs 0.70 mg/m^3). The low and high dose chrysotile aerosol exposures had 119 and 233 WHO f/cm^3 and 28 and 72 fibers(L > 20 µm)/cm^3, respectively. Similarly, the crocidolite and amosite asbestos groups were exposed to 181 and 281 WHO f/cm^3 and 24 and 48 fibers(L > 20 µm)/cm^3, respectively. The fiber characteristics of the chrysotile, crocidolite, and amosite exposure aerosols were therefore comparable.

The aerosolized chrysotile, crocidolite, and amosite fibers were all largely rat respirable. The bivariate size distribution in the exposure aerosol of each of the test substances has been presented in Bernstein et al. (2019a).

The brake dust was micronized to assure that it was rat respirable. In the brake dust exposed groups, between 91 and 99 % of the aerosol fibers were rat respirable (< 1 µm fiber diameter). For fibers ≥20 µm in length in the low dose brake dust group, 64 % were rat respirable, while in the mid and high dose groups, 91 and 86 % were rat respirable.

In the current study, more than 99 % of the chrysotile fibers (all lengths) present were rat respirable (< 1 μm diameter). For fibers > 20 μm in length, 99 % were also rat respirable. More than 98 % of the crocidolite fibers (all lengths) present were rat respirable (< 1 μm fiber diameter). For fibers > 20 μm in length, 96 % were also rat respirable. Similarly, for the amosite exposure group, 95 % of all fibers were rat respirable, and 95 % of the fibers L > 20 μm were also rat respirable.

The geometric mean diameter (and standard deviation) of the aerosol in each group are presented in Table 7. Each of the test substances was largely respirable in the rat and would have been respirable in humans (Miller, 1999).

The clearance half-time of the fibers in days was determined following the termination of the 90-day inhalation exposure. In the brake dust exposed groups (groups 2, 3, & 4), all chrysotile fibers L > 20 μm had cleared by 180 days. In the pure chrysotile exposure groups (groups 6 & 7) the fibers L > 20 μm cleared with $T_{1/2}$ of 23 and 37 days, respectively. The fibers L > 20 μm in the crocidolite and amosite exposure groups (groups 8 & 9) cleared with $T_{1/2}$ of 518 and 13,446 days, respectably. The clearance half-times for all fiber lengths have been presented in Table 4 of Bernstein et al. (2019a).

The mechanism by which chrysotile clears quickly from the lung has been postulated based upon the known physical and chemical properties of chrysotile. Chrysotile is a thin (7.4 angstoms) rolled sheet silicate with magnesium on the outside and silica on the inside (Whittaker, 1957, 1963; Tanji et al., 1984; Titulaer et al., 1993). Chrysotile is soluble in acid (Kobell, 1834). In addition, longer chrysotile fibers have been found to dissociate into short fibers of < 5 μm in length, which have been characterized as amorphous silica, in Gambles solution adjusted to the pH of the macrophage (Osmond-McLeod et al., 2011).

The rapid clearance of chrysotile is likely a result of the initial disassociation of deposited chrysotile bundles into fibrils through interaction with the lung surfactant at neutral pH. Subsequent breakage and dissolution then occurs through interaction with the alveolar macrophages at acidic pH.

There have been no studies performed to determine what effect might occur in this process if lung macrophage function is compromised in some individuals. The macrophage is a key element in the body's defense against bacterial and viral insults as well as in the clearance of foreign material in the lung (Hussell and Bell, 2014).

In COPD and asthma, the macrophage response has been reported to be altered (Ogger and Byrne, 2021). It seems that that the insults which result in these conditions, stimulate the production of the number of macrophage; however, these may be less effective in phagocytosis than normally. These macrophages have been reported to release their mediators, such as extracellularly secreted acid hydrolases, which attack the lung tissue (Davies and Allison, 1976). If these acidic mediators (Nathan, 1987; Nyberg et al., 1992) interact with long chrysotile fibers, the effect on these fibers would likely be similar to that which occurs when the macrophage attempts to phagocytize these fibers. In addition, neutrophils that are recruited in response have been shown to release acid hydrolases which could further facilitate the long chrysotile fiber disintegration (Unanue, 1976).

6.1. Histopathological examination

The results of the histopathological examination confirm that the response to the inhalation of brake dust with chrysotile is no different from a low dose insoluble particle (TiO_2) exposure and that such exposure does not produce a statically significant pathogenic or tumorigenic response in the lung.

During exposure (Bernstein et al., 2019b), the inhaled brake dust resulted in principally a macrophage response with associated particle-laden macrophage accumulation primarily at the bronchiolo-alveolar junctions. This response was similar or less than that observed for TiO_2 a “poorly soluble, low toxicity” (PSLT) particle (ECETOC-TR-122, 2013; Borm and Driscoll, 2019).

Table 5
At necropsy: macroscopically suspected visceral pleural lesions in the lung.

Exposure Group	Animal No	Slide ID	Histopathologic diagnosis	
			Lung parenchyma	Pleural lesion
Crocidolite Group 8	8070	30A	Carcinoma, bronchiolo-alveolar	No
		30B		No
		39		Focal very slight mesothelial hyperplasia
	8073	38	Adenoma, bronchiolo-alveolar	No
	8082	30C	Carcinoma, bronchiolo-alveolar	Focal very slight mesothelial hyperplasia
		38		No
	8097	29B	No correlation to possible macro lesion	Focal very slight mesothelial hyperplasia
		30B	Carcinoma, bronchiolo-alveolar	Focal very slight mesothelial hyperplasia and slight pleural fibrosis
		30C		Focal very slight mesothelial hyperplasia and slight pleural fibrosis
Amosite Group 9	9071	30C	No correlation to possible macro lesion	No
	9073	28C	Adenoma, bronchiolo-alveolar	No
	9080	38	Carcinoma, bronchiolo-alveolar	Multi-focal slight mesothelial hyperplasia
	9087	30B	Adenocarcinoma	No
		30C	Adenocarcinoma	No
	9090	29A	Carcinoma, bronchiolo-alveolar	Focal very slight mesothelial hyperplasia and slight pleural fibrosis
		30A	No correlation to possible macro lesion	No
		38	See slide 29A: Carcinoma, bronchiolo-alveolar	No
	9092	30B	Hyperplasia, bronchiolo-alveolar; alveolar type with atypia, focal severe	No
		39	Hyperplasia, bronchiolo-alveolar; alveolar type with atypia, focal severe	Focal very slight pl eu ral fibrosis
	9094	30A	Adenoma, bronchiolo-alveolar	No
	9096	38	Hyperplasia, bronchiolo-alveolar; alveolar type with atypia, focal severe	No
	9097	38	Adenoma, bronchiolo-alveolar	Focal adhesio n to thoracic wall
	9098	39	Adenoma, bronchiolo-alveolar	Foc al very slight pleural fibrosis
	9171	38	Carcinoma, bronchiolo-alveolar	No

Following termination of exposure, this macrophage response resolved over time. By 24 months, many of the animals in the brake dust groups ranged in response between Wagner grade 2 (a very slight dose-dependent incidence of particle-laden macrophages) and Wagner grade 1, similar to the air control (Tables 4 and 5). In the low dose brake dust group, out of 31 rats, 28 had returned to grade 1 (air control). A similar trend was observed in the TiO_2 particle control exposed animals.

As presented above, the Wagner grade is not very specific to the amount of a finding present, only that it was present. The histopathological examination further delineated the amount of each finding that was observed using the scale: None, very slight, slight, moderate, severe and very severe. In addition, for the presence of fibrosis which by the Wagner score would be 4, the above delineation was also performed (None, very slight, slight, moderate, severe and very severe), providing more detail and, in addition, a quantitative assessment of the amount of fibrosis (McConnell and Davis, 2002) as presented in Table 6. Within Wagner grade 4, very slight fibrosis corresponded to ~0.08 %; slight ~0.27 %; moderate ~0.4 %; severe ~ 1.0% of the lung with fibrosis. The slight and very slight fibrosis has been observed as an occasional finding that can resolve over time, while moderate and severe are persistent and have not been observed to resolve.

In the chrysotile exposed groups, very slight (multi)focal (minimal) alveolar/interstitial accumulation of particle-laden macrophages was seen primarily at bronchiole-alveolar junctions. Through 18 months, the Wagner grade ranged between 2 and 3 with single rats with very slight interstitial fibrosis (Wagner grade 4, fibrotic quantification of 0.08–0.27 % of the lung) at 6, 12, and 24 months. By 24 months in the low dose chrysotile, out of 31 rats, 12 had a Wagner grade of 1, 18 a grade of 2 and 1 a grade of 3. In the high dose chrysotile, out of 31 rats, 4 had a Wagner grade of 1, 14 a grade of 2 and 12 a grade of 3 and 1 a grade of 4.

Following exposure to crocidolite and amosite very slight to slight multifocal, (minimal) alveolar/interstitial accumulation of fiber-laden macrophages (alveolar histiocytosis), was observed primarily at bronchiolo-alveolar junctions. This was associated with multifocal infiltration in the peribronchial/peribronchiolar and alveolar/interstitial (intraseptal) regions of inflammatory cells (mixed) with at the bronchiolo-alveolar junctions slight multi-focal microgranulomas. Multifocal interstitial fibrosis (slight – very slight) was seen in all rats over all time points through 24 months. This corresponded to a Wagner grade of 4 which was seen in all amphibole asbestos-exposed rats at all time points.

6.1.1. Neoplastic findings

Through the 90-day inhalation exposure and the post-exposure period of up to 24 months, no exposure-related neoplastic findings were observed. At the end of the post-exposure period (24 months) only group 8 (crocidolite) and group 9 (amosite), exhibited an increased number of lung tumors as compared to the air control, TiO_2, and brake dust exposed groups.

The tumors mainly consisted of adenomas and carcinomas of the bronchiolo-alveolar type. Mesotheliomas or preneoplastic pleural lesions were not detected in the thoracic cavity, including lung (visceral) and thoracic wall (parietal) pleura. Only one mesothelioma was observed in the abdominal cavity of one animal of group 8, which was interpreted to be unrelated to the inhalation. In this animal, the mesothelioma was only observed in the abdominal cavity and tunica vaginalis. No tumor cells were observed in the thoracic cavity, pleura, lung, or lung-associated lymph nodes. Therefore, this tumor was interpreted to be an incidental background finding. The tunica vaginals of the testis represents a predilection site for mesotheliomas in male Wistar rats. The mesotheliomas arising at this site spread throughout the whole abdominal cavity. The mesothelioma observed in the study was found only in the abdominal cavity, including the tunica vaginalis of the testis. No concurrent lesions were seen in the thorax. Therefore, the mesothelioma of the abdominal cavity was interpreted to be unrelated to the inhalation.

Table 6
Fibrosis quantification performed by Fraunhofer on histopathology slides (shown is the percentage of the number of grids on the slide with fibrosis reflecting the presence/intensity of the fibrotic response).

Group	45 days	89 days (end of exposure)	180 days	6 months	12 months	18 months
Brake dust low, med, high	0	0	0	0	0	0
TiO_2	0	0	0	0	0	0
Chrysotile low dose	0	0	0	0.08	0	0
Chrysotile high dose	0	0.28	0	0.27	0	0
Crocidolite	0.43	0.75	1.05	1.07	0.96	0.96
Amosite	0.77	0.99	1.10	1.10	1.05	1.05

The treatment-related findings (macrophage response) decreased in their severity during the post-exposure period in groups 2–7 through the 24 months post-exposure period. The decline of the severity is also reflected by a reduced Wagner grade of the animals of group 2–7. However, in groups 8 and 9, the severity of the treatment-related findings, including the Wagner grade, remained elevated during the 24 months post-exposure period, and the tumor response appeared to be dose-related.

6.1.2. Bronchiolo-alveolar hyperplasia

In the lungs, the only non-neoplastic epithelial change observed was multifocal bronchiolo-alveolar hyperplasia (bronchiolar type) (synonym: alveolar bronchiolization). Such hyperplasia is characterized by the presence within alveolar ducts and adjacent alveoli of the bronchiolar epithelium (bronchiolisation). It is frequently observed following particle and/or fiber inhalation and is considered as a mechanism by which the lung tries to facilitate the removal of particle and/or fiber through the extension of the "mucociliary escalator".

Alveolar bronchiolization is not considered a preneoplastic lesion, even if graded severe. In the current study, alveolar bronchiolization was graded no more than very slight to slight in any group or at any time point.

Other types of epithelial hyperplasia, such as bronchiolo-alveolar hyperplasia of the alveolar type (alveolar type II cell hyperplasia) or bronchiolo-alveolar hyperplasia of the mixed type (mixture of bronchiolar and alveolar type II cells), which at a severe degree are of more concern regarding a potential preneoplastic character were observed at low levels in all groups but were increased in the chrysotile high, crocidolite and amosite group. The same refers to epithelial cell metaplasia, e.g., squamous cell metaplasia.

The bronchiolar-alveolar hyperplasia of the alveolar type (alveolar type II cell hyperplasia) is slightly increased in the chrysotile high dose group. These lesions are considered to be preneoplastic if they are graded severe. However, the increased bronchiolar-alveolar hyperplasia of the alveolar type in the chrysotile high-dose group were only very slight, slight or moderate. Concerning the bronchiolar-alveolar hyperplasia of the bronchiolar type, there are per se not considered to be preneoplastic. These hyperplasias are characterized by ciliated cells. It is generally believed that solid adenomas are composed of cells expressing alveolar Type II cell features and are therefore considered benign alveolar Type II cell tumors. Papillary adenomas, however, are considered either to be less well-differentiated Type II cell tumors progressing toward a malignant phenotype or to be of club cell origin. Therefore, the bronchiolar-alveolar hyperplasias of the bronchiolar type are not considered to be a progenitor of the bronchiolo-alveolar adenomas (Renne et al., 2009).

There was no occurrence histologically of mesothelial cell hyperplasia (proliferation of pleural mesothelial cells) in groups 1–7 in the present study. In the amphibole asbestos-exposed groups (8 & 9), histopathological examination of the macroscopically suspected visceral pleural lesions in the lung showed that the macroscopic changes correlated with bronchiolo-alveolar carcinoma, bronchiolo-alveolar adenoma or bronchiolo-alveolar hyperplasia (alveolar type with atypia) in the lung parenchyma. The lesions in the overlying lung visceral pleura consisted of multi-focal very slight to slight mesothelial (visceral pleural) hyperplasias and/or pleural fibrosis. One animal, animal 9097, showed an adhesion of the lung pleura to the thoracic wall

(Figure Section S-3.4, Picture 178, Supplemental data).

The confocal microscopy examination showed that there was increased collagen on both the visceral and parietal pleura as well as increased mesothelial thickness. The confocal images also showed the presence of adhesions of the lung pleura to the thoracic wall.

6.2. Inflammation and tumorigenesis

As presented above, tumors within the lung were detected in the groups clean air (one tumor), brake dust high (one tumor), titanium dioxide (one tumor), chrysotile low (one tumor), crocidolite (five tumors), and amosite (nine tumors). The tumors in the crocidolite and amosite exposure groups were considered to be exposure-related.

This is further confirmed by the role of inflammation in the pathogenesis of lung cancer. Chronic inflammation is associated with the development of cancer (Hanahan and Weinberg, 2011; Conway et al., 2016). In contrast to acute inflammation that is important for clearing infection, healing wounds, and maintaining tissue homeostasis, inflammation associated with tumor development is often low in grade and chronic (Yang and Lin, 2017). With fiber-related inflammation and carcinogenesis, long durable fibers such as the crocidolite and amosite fibers in this study, once inhaled, are present as physical impediments, which the macrophage fails to successfully phagocytize and clear. With such fibers, the frustrated phagocytosis releases the proteolytic enzymes, which can break down the connective tissue of the lung (Fels and Cohn, 1986). Grecian et al. (2018) and Michel et al. (2013) have reviewed the relationship of the cross-talk between macrophages and natural killer cells such as neutrophils and the role of neutrophils in cancer.

The lack of inflammation and pathogenesis in the control and brake dust groups and the lack of persistence in response in the chrysotile groups, which largely resolved by 24 months, provides a further explanation as to why the exposures in these groups did not produce a carcinogenic response in this study.

6.3. Confocal imaging and collagen quantification

In addition to the histopathological differentiation of the response to brake dust, TiO_2 and chrysotile in comparison to crocidolite and amosite asbestos, the quantification of fibrosis both histopathologically and by confocal microscopy and imaging provides further confirmation that brake dust with chrysotile does not initiate events that lead to carcinogenesis.

A semi-qualitative analysis of the amount of fibrosis in the lung was performed by the pathologist. A grid of 100 μm × 100 μm size was overlaid on the tissue (each square was 10,000 μm^2 or 0.01 mm^2). A square was considered positive if interstitial fibrosis was observed consistent with a Wagner grade 4 or higher (Table 6). If not it was considered negative. This assessment provided a semi-quantitative determination of the absence or presence of collagen in each of the squares assessed, although not the total amount.

The confocal microscopy analysis included in this study provides detailed quantification of the amount of collagen (fibrosis) in the lung parenchyma as well as the visceral and parietal pleura. The confocal 3D images allow definition of preneoplastic changes in the pleural cavity, which have been associated with mesothelioma in humans. In these images, the color-coding of tissues, macrophages, and other inflammatory cells such as neutrophils in various shades of green, with the brightest green indicative of connective tissue and excess collagen. The amount of collagen present was directly proportional to the intensity of the green images (Rogers, 1999). For each animal in order to obtain the necessary quantitative information, more than 12,000 confocal micrographs were recorded and analyzed. For the collagen determination for each time point, a total of more than 432,000 images were recorded.

Through the final results of this study, the confocal analysis has continued to support the results observed through the histopathological examination. The additional precision and quantification provided by the confocal 3D images in the assessment of possible fibrotic response provide valuable insight into the translocation of fibers within the lung and to the pleural cavity and the relationship of fiber type to disease. The confocal examination also quantified the presence and length of fibers and clearly showed that only the amphibole fibers, crocidolite, and amosite, resulted in a persistent increase of mesothelial thickness and visceral and parietal pleura collagen. In addition, the confocal imaging showed the presence of amphibole fibers in the pleural cavity as well as the development of pleural adhesions.

6.4. Comparison with historical inhalation studies

Wagner et al. (1974) reported a range of different inhalation studies of asbestos in rats that included a group with 3 months exposure followed by life-time observation. The asbestos samples used consisted of the 5 UICC standard reference samples (Timbrell et al., 1968). The UICC samples were heavily ground, which resulted in a large proportion of particles and short fibers (Bernstein, 2015). The exposures were reported as ranging from 10 to 14 mg/m^3 respirable concentration. There was no mention of the percent that was respirable or of the total aerosol concentration generated in these studies. Groups of rats were exposed for either 1 day, 3, 6, 12 or 24 months. Exposures were at a single high dose (no dose-response).

It has been estimated based on studies by Mast et al. (1995a, 1995b), which also used UICC samples and measured fiber concentration by TEM, that exposures of 10 mg/m^3 resulted in more than 100,000 total f/cm^3 in the aerosol. Mast et al., did not report the non-fibrous particles that were present, likely in very high concentrations as a result of the grinding of the UICC fiber sample and the aerosol generation system used. While both lung tumors and mesotheliomas were produced at these exposure concentrations, anomalies were also reported. As an example, Wagner stated that "First, in Experiment 1 two mesotheliomata occurred with the one day exposure compared with only one with the 3 months' exposure, which had a (sic cumulative) dosage more than 50 times greater." The lung and mesothelioma tumor response in the Wagner study is shown in Table 8. There is little association with cumulative exposure for either the amphibole or chrysotile asbestos

Table 7
Geometric mean diameter (GMD) and geometric standard deviation (GSD) of the aerosol in each group.

Exposure group	GMD (μm) (GSD)
(Group 1) Air Control	0.27 (1.89)
(Group 2) Brake dust – low dose	0.15 (1.88)
(Group 3) Brake dust – mid dose	0.16 (1.73)
(Group 4)** Brake dust – high dose	0.15 (1.91)
(Group 5)*** Titanium dioxide	0.23 (1.77)
(Group 6) Chrysotile – low dose	0.11 (1.86)
(Group 7) Chrysotile – high dose	0.11 (1.85)
(Group 8) Crocidolite – high dose	0.24 (1.80)
(Group 9) Amosite – high dose	0.28 (1.80)

** For the brake dust group 4, the MMAD = 2.6 μm (geometric standard deviation = 2.54) as determined by the impactor measurement.

*** The geometric mean diameter of the TiO_2 particles as determined by SEM was 0.39 μm (below the lower cut-off of the impactor).

Table 8
Tumour response from Wagner et al. (1974).

Fiber	Exposure duration	% lung tumours	% mesothelioma
Amosite	1 day	27	2
Amosite	3 months	27	0
Amosite	6 months	11	0
Amosite	12 months	40	0
Amosite	24 months	61	0
Crocidolite	1 day	14	2
Crocidolite	3 months	39	3
Crocidolite	6 months	22	0
Crocidolite	12 months	69	8
Crocidolite	24 months	72	0
Chrysotile	1 day	2	0
Chrysotile	3 months	53	0
Chrysotile	6 months	29	0
Chrysotile	12 months	47	13
Chrysotile	24 months	47	5
Control	1 day	9	0
Control	3 months	8	0
Control	6–24 months	0	0

groups.

The high particle and short fiber aerosol concentrations used in these studies likely resulted in lung overload[7]. It is estimated that approximately 90 fibers were deposited in each of the 40,000,000 alveoli in the lung per day (Pinkerton et al., 1992; Bernstein, 2007). As distribution is not uniform, many alveoli would receive considerably more per day. Under such conditions, it would be difficult to imagine that normal macrophage function can take place, which is integral to the clearance of chrysotile fibers.

Most other historical inhalation toxicology studies of asbestos were of 12 or 24-month exposure duration. These studies, however, also used similar fiber sources, aerosol generation techniques and very high exposure concentrations, which would likely result in lung overload (Bernstein, 2015).

The biopersistence/clearance of the brake dust from brakes manufactured with chrysolite (Bernstein et al., 2015) has demonstrated that the biosolubility of chrysotile results in breakage and accelerated clearance and lack of toxicity in comparison to the amphibole asbestos crocidolite. The mineralogical structure of chrysotile and the mechanisms by which components leach and lead to dissolution and fragmentation following inhalation have been presented by Poland (2019).

The structure of chrysotile is that of a thin rolled sheet with the magnesium on the outside of the curl and the silica on the inside, which facilitates it being acid soluble (Titulaer et al., 1993; Tanji et al., 1984; Whittaker, 1963; Whittaker, 1957; Kobell, 1834;) and not biopersistent. The present study demonstrates this through the absence of a sustained fibrogenic response and no significant increase in lung tumors.

The structure of amphibole asbestos fibers, such as crocidolite and amosite, are markedly different. With amphiboles, the silica is on the outside, forming an impermeable encasement. The amphibole fibers are insoluble at any pH that occurs in physiological conditions (Whittaker, 1960; Skinner et al., 1988). Upon inhalation, amphibole fibers which are long enough to frustrate clearance by the macrophage will persist in the lung and, as seen in this study (Bernstein et al., 2019a, 2019b & this publication) will quickly induce a persistent inflammatory response which leads to continued tissue injury, resulting in fibrogenic response and dose-dependent lung tumors. As shown in Table 3, the tumorigenic potential in the lung of the crocidolite and amosite asbestos was associated with the number of fibers L > 20 μm/cm^3 in the aerosol and not with the total particle/fiber concentration/cm^3.

The chrysotile aerosol exposure concentrations in this study were 119 and 233 f (WHO)/cm^3 (0.27 and 0.64 mg/m^3, Grps 6–7, respectively). These concentrations were 2975–5825 times the mean historical brake dust exposure TWA and 50–175 times the concentrations used in the brake dust exposed groups (Grps 2–4). As seen in this study, the response to chrysotile, even at these concentrations, is largely that of a poorly soluble dust such as TiO_2. In contrast, the amphibole asbestos crocidolite and amosite produced, at comparative exposure concentrations of 181 and 281 f (WHO)/cm^3 (1.28 and 2.32 mg/m^3, Grps 8 & 9, respectively), a continuum of fiber-related pathology leading to interstitial fibrosis and lung tumors as well as pleural mesothelial activation, pleural fibrosis, and pleural adhesions.

The exposure concentrations in this study were considerably greater than in historical brake dust with chrysotile exposures and clearly differentiated the lack of tumorigenic potential in the lung of brake dust compared to amphibole asbestos. While the cumulative dose of either crocidolite or amosite was not sufficient to produce mesothelioma, the confocal microscopy has shown that it was sufficient to provide early indicators of mesothelial pathological response in the pleura, including increased visceral and parietal pleura collagen, an increased thickness of the mesothelial layer, as well as pleural adhesions, which are early indicators of mesotheliogenic response, if sustained.

7. Conclusion

The final results from this 90-day multi-dose inhalation toxicology study with life-time post-exposure observation have shown a significant fundamental difference in pathological response and tumorgenicity between brake dust generated from brake pads manufactured with chrysotile or from chrysotile alone in comparison to the amphiboles, crocidolite, and amosite asbestos.

The confocal imaging and quantitative collagen assessment in conjunction with the standard bronchoalveolar lavage and histopathological examination provided improved understanding and characterization of the pulmonary response to brake dust with chrysotile as compared to TiO_2, chrysotile alone or crocidolite or amosite asbestos in the lung and the pleural cavity.

In the groups exposed to brake dust which contained chrysotile, there was no sustained fibrotic response and no excess lung tumors compared to the air control group at exposure concentrations well above those at which humans have been exposed. A slight accumulation of particles laden macrophages was noted in response to the high dose brake dust exposure. The Wagner grade showed a non-dose dependent response ranging from 1 to 2 (with 1 being the response in the air control group). The TiO_2 exposed group showed similar scores.

Chrysotile fibers were not biopersistent, exhibiting in the lung a deterioration of their matrix which results in breakage into particles and short fibers which can be cleared by alveolar macrophages and which can continue to dissolve. Particle-laden macrophage accumulation was noted in both chrysotile exposure groups leading to a slight interstitial inflammatory response. There was no peribronchiolar inflammation and occasional very slight interstitial fibrosis in single rats. Wagner grades were largly 1–3 with occasional single rats 4. No exposure related tumors were observed in either dose.

In the crocidolite and amosite asbestos-exposed groups, elevated neutrophils (BAL), persistent inflammation, microgranulomas, and fibrosis (Wagner grade 4) were observed during the exposure. The inflammation, microgranulomas, and fibrosis persisted through the post-exposure period and were associated with a dose-response incidence of lung tumors.

The response to amphibole asbestos was also clearly differentiated through the confocal microscopy of the lung and snap-frozen chestwalls. Extensive inflammatory response was observed, and significant collagen development both in the lung and on the visceral and parietal surfaces

[7] Lung overload has been shown to occur following inhalation of high concentrations of insoluble nuisance dusts. These high concentrations, compromise the lung's clearance mechanisms by reducing macrophage function and associated clearance. This has been shown in the rat to produce inflammation and a tumorigenic response (Oberdörster, 1995; Morrow, 1992; Morrow, 1988; Muhle et al., 1988; Bolton et al., 1983).

was quantified. A significant increase in mesothelial thickness was also observed on both the visceral and parietal surfaces as well as pleural adhesions.

This study is also unique in that it establishes that when the fiber characteristics and dose are carefully determined, and appropriate inhalation exposure is taken into account correctly, the inhalation model provides the most sensitive relationship of fiber dose-response and the only physiological method reproducing real-world exposures for evaluating potential fiber toxicity and tumorigenicity.

The results reported here, based on these guiding principles, provide a clear foundation for differentiating the innocuous effects of brake dust exposure from the adverse effects following amphibole asbestos exposure.

8. Study limitations

This study was performed in rats which, in comparison to humans, are mandatory nasal breathers. The exposure aerosols were determined to be respirable in the rats and would also have been respirable in humans. The lung architecture in the rat is monopodial, while that of humans is bipodia-tripodial (Miller, 1999). The macrophage of the rat has been reported to be smaller than that of humans (Miller, 2000). The doses used in this study exceeded those to which brake workers have been exposed. While the doses were much lower than those used in previous studies (e.g., Wagner et al., 1974) the current state of art for inhalation studies would not use such high doses due to lung overload effects (Oberdörster, 1995).

Declaration of Competing Interest

This study was funded by Honeywell International Inc. All protocol, design of the experimental procedures, and the choice of laboratories was performed by D.M. Bernstein in conjunction with the scientific advisory board (see acknowledgments, below). The laboratory work to Citoxlab (currently Charles River Laboratories Hungary), Fraunhofer Institute, GSA, and Rogers Imaging was sub-contracted by D.M. Bernstein. The affiliations of the authors are as shown on the cover page and include research laboratories, a government institute, corporate affiliations, as well as an independent toxicology consultant. This publication is the professional work product of the authors and may not necessarily represent the views of the corporate sponsor. One of the authors, David Bernstein, has appeared as an expert witness in litigation concerned with alleged health effects of exposure to chrysotile. Honeywell is a defendant in asbestos-product litigation, and its predecessor manufactured the automotive brakes used in this study. There have been periodic communications between Honeywell and the authors concerning the status of this study. The contribution of Prof JI Phillips is based on research supported by the National Research Foundation.

Acknowledgements

The authors wish to acknowledge the excellent contribution to the design and conduct of this study of Drs. Vincent Castranova, Annie M. Jarabek, Ernest E. McConnell and Günter Oberdörster who served as members of an independent scientific advisory board to this study.

We would also like to acknowledge the members of the pathology review board Drs. Dirk Schaudien, Heinrich Ernst, Gene McConnell, Vince Castranova, Annie Jarabek, Günter Oberdörster, Ron Herbert; Jim Phillips; Rick Rogers, David Bernstein who provided a thorough and independent review and consensus of the preneoplastic and neoplastic findings in this study. The final report provided by Dr. Dirk Schaudien of the Fraunhofer Institute fully reflects this consensus.

We also wish to acknowledge the excellent work of the inhalation technical group staff at Charles River Laboratories Hungary: András Bálint, Zoltán Jónás, Imre Bíró, Huba Szabó, Dániel Zentai-Papp, Zoltán Németh, Dániel Németh, László Ács and the necropsy group members: Ferenc Szűcs, Henrietta Miklós, Hajnalka Lovasi, István Róka in the performance of this study. We would also like to thank Stephane Gaering for his expertise and technical assistance. Finally, we would like to thank Talis Reks and David Kling of Rogers Imaging Corp. for their excellent work with the confocal imaging and data collection.

Appendix A. Supplementary data

Supplementary data to this article can be found online at https://doi.org/10.1016/j.taap.2021.115598.

References

Bernstein, D.M., 2007. Synthetic vitreous fibers: a review toxicology, epidemiology and regulations. Crit. Rev. Toxicol. 37 (10), 839–886.

Bernstein, D.M., 2015. Serpentine and amphibole asbestos. In: Salem, H., Katz, S. (Eds.), Inhalation Toxicology, 3rd ed. Taylor & Francis Group, Boca Raton, FL, pp. 295–326 (Chapter 14) ISBN 9781466552739.

Bernstein, D.M., Pavlisko, E.N., 2017. Differential pathological response and pleural transport of mineral fibres. In: EMU Notes in Mineralogy, Vol. 18, pp. 417–434. https://doi.org/10.1180/EMU-notes.18.12 (Chapter 12) Copyright 2017 the European Mineralogical Union and the Mineralogical Society of Great Britain & Ireland.

Bernstein, D.M., Rogers, R., Sepulveda, R., Kunzendorf, P., Bellmann, B., Ernst, H., Phillips, J.I., 2014. Evaluation of the deposition, translocation and pathological response of brake dust with and without added chrysotile in comparison to crocidolite asbestos following short-term inhalation: Interim results. Toxicol. Appl. Pharmacol. 276 (1), 28–46.

Bernstein, D.M., Rogers, R., Sepulveda, R., Kunzendorf, P., Bellmann, B., Ernst, H., Creutzenberg, O., Phillips, J., 2015. Evaluation of the fate and pathological response in the lung and pleura of brake dust alone and in combination with added chrysotile compared to crocidolite asbestos following short-term inhalation exposure. Toxicol. Appl. Pharmacol. 283, 20–34.

Bernstein, D.M., Toth, B., Rogers, R., Sepulveda, R., Kunzendorf, Phillips, J., Ernst, H., 2018. Evaluation of the dose-response and fate in the lung and pleura of chrysotile-containing brake dust compared to chrysotile or crocidolite asbestos in a 28-day quantitative inhalation toxicology. study will be published in Toxicol. Appl. Pharmacol. 351, 74–92.

Bernstein, D.M., Toth, B., Rogers, R.A., Kling, D., Kunzendorf, P., Phillips, J.I., Ernst, H., 2019a. Evaluation of the exposure, dose-response and fate in the lung and pleura of chrysotile-containing brake dust compared to TiO2, chrysotile, crocidolite or amosite asbestos in a 90-day quantitative inhalation toxicology study – interim results Part 1: experimental design, aerosol exposure, lung burdens and BAL. Toxicol. Appl. Pharmacol. 387, 2020 Jan 15. 114856.

Bernstein, D.M., Toth, B., Rogers, R.A., Kling, D., Kunzendorf, P., Phillips, J.I., Ernst, H., 2019b. Evaluation of the dose-response and fate in the lung and pleura of chrysotile containing brake dust compared to TiO2, chrysotile, crocidolite or amosite asbestos in a 90-day quantitative inhalation toxicology study – Interim results Part 2: Histopathological examination, Confocal microscopy and collagen quantification of the lung and pleural cavity. Toxicol. Appl. Pharmacol. 387, 2020 Jan 15. 114847.

Blau, P.J., 2001. Compositions, Functions, and Testing of Friction Brake Materials and Their Additives. N. p., United States https://doi.org/10.2172/788356.

Bolton, R.E., Vincent, J.H., Jones, A.D., et al., 1983. An overload hypothesis for pulmonary clearance of UICC amosite fibers inhaled by rats. Br. J. Ind. Med. 40, 264–272.

Borm, P.J.A., Driscoll, K.E., 2019. The hazards and risks of inhaled poorly soluble particles – where do we stand after 30 years of research? Part Fibre Toxicol. 16, 11.

Campbell, I., 2007. Chi-squared and Fisher-Irwin tests of two-by-two tables with small samplerecommendations. Stat. Med. 26, 3661–3675.

Conway, E.M., Pikor, L.A., Kung, S.H.Y., Hamilton, M.J., Lam, S., Lam, W.L., Bennewith, K.L., 2016. Macrophages, Inflammation, and lung cancer. Am. J. Respir. Crit. Care Med. 193 (2), 116–130, 2016 Jan 15.

Davies, P., Allison, A.C., 1976. The macrophage as a secretory cell in chronic inflammation. Agents Actions 6 (1/2/3), 60–74. Birkhauser Verlag, Basel.

ECETOC, 2013. ECETOC technical report No. 122. In: Poorly Soluble Particles/Lung Overload, European Centre for Ecotoxicology and Toxicology of Chemicals, Brussels, Belgium.

Fels, A.O., Cohn, Z.A., 1986. The alveolar macrophage. J. Appl. Physiol. 60 (2), 353–369. Feb.

Grecian, R., Whyte, M.K.B., Walmsley, S.R., 2018. The role of neutrophils in cancer. Br. Med. Bull. 128 (1), 5–14, 2018 Dec 1.

Hanahan, D., Weinberg, R.A., 2011. Hallmarks of cancer: the next generation. Cell 144 (5), 646–674. Mar 4.

Hussell, T., Bell, T., 2014. Alveolar macrophages: plasticity in a tissue-specific context. Nat. Rev. Immunol. 14, 81–93. https://doi.org/10.1038/nri3600.

IARC, 2010. Monographs on the Evaluation of Carcinogenic Risks to Humans VOLUME 93 Carbon Black, Titanium Dioxide, and Talc, World Health Organization International Agency For Research On Cancer IARC. WHO Press, Geneva.

Kobell, F., 1834. Ueber den schillernden Asbest von Reichenstein in Schlesien. J. Prakt. Chem. 2, 297–298.

Macklin, C.C., 1955. Pulmonary sumps, dust accumulations, alveolar fluid and lymph vessels. Acta Anat. (Basel) 23 (1), 1–33.

Margaris, K., Black, R.A., 2012. Modelling the lymphatic system: challenges and opportunities. J. R. Soc. Interface 9 (69), 601–612.
Mast, R.W., McConnell, E.E., Anderson, R., Chevalier, J., Kotin, P., Bernstein, D.M., Thevenaz, P., Glass, L.R., Miiller, W.C., Hesterberg, T.W., 1995a. Studies on the chronic toxicity (inhalation) of four types of refractory ceramic fiber in male Fischer 344 rats. Inhal. Toxicol. 7, 425–467.
Mast, R.W., McConnell, E.E., Hesterberg, T.W., Chevalier, H.J., Kotin, P., Thevenaz, P., Bernstein, D.M., Glass, L.R., Miiller, W., Anderson, R., 1995b. A multiple dose chronic inhalation toxicity study of size-separated kaolin Refractory Ceramic Fibers (RCF) in Male Fischer 344 rats. Inhal. Toxicol. 7 (4), 469–502.
McConnell, E.E., Davis, J.M., 2002 Mar.. Quantification of fibrosis in the lungs of rats using a morphometric method. Inhal. Toxicol. 14 (3), 263–272.
McConnell, E.E., Wagner, J.C., Skidmore, J.W., Moore, J.A., 1984. A comparative study of the fibrogenic and carcinogenic effects of UICC Canadian chrysotile B asbestos and glass microfibre (JM 100). In: Biological Effects of Man-Made Mineral Fibres: Proceedings of a WHO/IARC Conference in Association with JEMRB and TIMA, Copenhagen, 2-22 April 1982, Vol. 2. WHO, Copenhagen, pp. 234–252.
Michel, T., Hentges, F., Zimmer, J., 2013. Consequences of the crosstalk between monocytes/macrophages and natural killer cells. Front. Immunol. 3, 403, 2013 Jan 4.
Miller, F.J., 1999. Dosimetry of particles in laboratory animals and humans. In: Hayes, A. W., Thomas, J.A., Gardner, D.E. (Eds.), Toxicology of the Lung, 3rd ed. Taylor & Francis, Philadelphia, pp. 513–555.
Miller, F.J., 2000. Dosimetry of particles in laboratory animals and humans in relationship to issues surrounding lung overload and human health risk assessment: a critical review. Inhal. Toxicol. 12 (1–2), 19–57. https://doi.org/10.1080/089583700196536. Jan–Feb.
Morrow, P.E., 1988. Possible mechanisms to explain dust overloading of the lung. Fundam. Appl. Toxicol. 10, 369–384.
Morrow, P.E., 1992. Dust overloading of the lungs: update and appraisal. Toxicol. Appl. Pharmacol. 113, 1–12.
Muhle, H., Bellman, B., Heinrich, U., 1988. Overloading of lung clearance during chronic exposure of experimental animals to particles. Ann. Occup. Hyg. 32 (Suppl. 1), 141–147.
Nathan, C.F., 1987. Secretory products of macrophages. J. Clin. Invest. 79 (2), 319–326. https://doi.org/10.1172/JCI112815, 1987 Feb.
Negrini, D., Moriondo, A., 2013. Pleural function and lymphatics. Acta Physiol (Oxford) 207, 244–259.
NIOSH, 1994 (2003). NIOSH Manual of Analytical Methods. Schlecht PCOC, P.F., editor. DHHS (NIOSH) Publication, pp. 94–113. http://www.cdc.gov/niosh/nmam/.
Nyberg, K., Johansson, U., Johansson, A., Camner, P., 1992. Phagolysosomal pH in alveolar macrophages. Environ. Health Perspect. 97, 149–152. https://doi.org/10.2307/3431344.
Oberdörster, G., 1995. Lung particle overload: implications for occupational exposures to particles. Regul. Toxicol. Pharmacol. 21, 123–135.
OECD 413, 2018. Test No. 413: Subchronic Inhalation Toxicity: 90-day Study, OECD Guidelines for the Testing of Chemicals, Section 4, Health Effects. https://www.oecd-ilibrary.org/environment/test-no-413-subchronic-inhalation-toxicity-90-day-study_9789264070806-en.
Ogger, P.P., Byrne, A.J., 2021. Macrophage metabolic reprogramming during chronic lung disease. Mucosal Immunol. 14, 282–295. https://doi.org/10.1038/s41385-020-00356-5.
Osmond-McLeod, M.J., Poland, C.A., Murphy, F., et al., 2011. Durability and inflammogenic impact of carbon nanotubes compared with asbestos fibres. Part Fibre Toxicol. 8, 15. https://doi.org/10.1186/1743-8977-8-15.
Pinkerton, K.E., Gehr, P., Crapo, J.D., 1992. Treatise on Pulmonary Toxicology, Vol. 1, Comparative Biology of the Normal Lung. CRC Press, Boca Raton, FL.
Poland, C.A., 2019. Duffin R the toxicology of chrysotile-containing brake debris: implications for mesothelioma. Crit. Rev. Toxicol. 15, 1–25. Mar.
Randall, T.D., 2010. Bronchus-Associated Lymphoid Tissue (BALT) structure and function. Adv. Immunol. 107, 187–241.
Renne, R., Brix, A., Harkema, J., Herbert, R., Kittel, B., Lewis, D., March, T., Nagano, K., Pino, M., Rittinghausen, S., Rosenbruch, M., Tellier, P., Wohrmann, T., 2009. Proliferative and nonproliferative lesions of the rat and mouse respiratory tract. Toxicol. Pathol. 37 (7 Suppl), 5S–73S. https://doi.org/10.1177/0192623309353423. Dec.
Rhee, S.K., 1974. Wear mechanisms for asbestos-reinforced automotive friction materials. Wear 29 (3), 391–393.
Richardson, J.T.E., 2011. The analysis of 2 x 2 contingency tables – yet again. Stat. Med. 30, 890.
Rogers, R.A., 1999. In situ microscopic analysis of asbestos and synthetic vitreous fibers retained in hamster lungs following inhalation. Environ. Health Perspect. 107, 367–375.
Semmler-Behnke, M., Takenaka, S., Fertsch, S., Wenk, A., Seitz, J., Mayer, P., Oberdörster, G., Kreyling, W.G., 2007. Efficient elimination of inhaled nanoparticles from the alveolar region: evidence for interstitial uptake and subsequent reentrainment onto airways epithelium. Environ. Health Perspect. 115 (5), 728–733.
Skinner, H.C.W., Ross, M., Frondel, C., 1988. Asbestos and Other FibrousMaterials — Mineralogy, Crystal Chemistry, and Health Effects. Oxford University Press, New York (NY).
Tanji, T., Yada, K., Akatsuka, Y., 1984. Alternation of clino- and orthochrysotile in a single fiber as revealed by high-resolution electron microscopy. Clay Clay Miner. 32 (5), 429–432.
Timbrell, V., Gibson, J.C., Webster, I., 1968 May 15. 1968 UICC standard reference samples of asbestos. Int. J. Cancer 3 (3), 406–408.
Titulaer, M.K., van Miltenburg, J.C., Jansen, J.B.H., et al., 1993. Characterization of tubular chrysotile by thermoporometry, nitrogen sorption, drifts, and TEM. Clay Clay Miner. 41, 496–513.
Unanue, E.R., 1976. Secretory function of mononuclear phagocytes: a review. Am. J. Pathol. 83 (2), 396–417.
Wagner, J.C., Berry, G., Skidmore, J.W., Timbrell, V., 1974. The effects of the inhalation of asbestos in rats. Br. J. Cancer 29 (3), 252–269, 1974 Mar.
Whittaker, E.J.W., 1957. The structure of chrysotile. V. Diffuse reflexions and fiber texture. Acta Crystallogr. 10, 149–156.
Whittaker, E.J.W., 1960. The crystal chemistry of the amphiboles. Acta Crystallogr. 13, 291–298.
Whittaker, E.J.W., 1963. Research report: Chrysotile fibers – filled or hollow tubes? Mathematical interpretation may resolve conflicting evidence. Chem. Eng. News 41, 34–35. September 30, 1963.
WHO, 1985. In: WHO/EURO MMMF Reference Scheme (Ed.), Reference Methods for Measuring Airborne Man-Made Mineral FibreFibers (MMMF). World Health Organisation, Copenhagen, 55 pp.
Yang, L., Lin, P.C., 2017 Dec. Mechanisms that drive inflammatory tumor microenvironment, tumor heterogeneity, and metastatic progression. Semin. Cancer Biol. 47, 185–195.